TECHNICAL REPORT ARBRL-TR-02457

SENSITIVITY ANALYSIS FOR PREMIXED, LAMINAR, STEADY-STATE FLAMES

Terence P. Coffee
Joseph M. Heimerl

January 1983

US ARMY ARMAMENT RESEARCH AND DEVELOPMENT COMMAND
BALLISTIC RESEARCH LABORATORY
ABERDEEN PROVING GROUND, MARYLAND

Destroy this report when it is no longer needed.
Do not return it to the originator.

Secondary distribution of this report is prohibited.

Additional copies of this report may be obtained from the National Technical Information Service, U. S. Department of Commerce, Springfield, Virginia 22161.

The findings in this report are not to be construed as an official Department of the Army position, unless so designated by other authorized documents.

The use of trade names or manufacturers' names in this report does not constitute indorsement of any commercial product.

UNCLASSIFIED

SECURITY CLASSIFICATION OF THIS PAGE *(When Date Entered)*

REPORT DOCUMENTATION PAGE		READ INSTRUCTIONS BEFORE COMPLETING FORM
1. REPORT NUMBER Technical Report ARBRL-TR-02457	2. GOVT ACCESSION NO.	3. RECIPIENT'S CATALOG NUMBER
4. TITLE *(and Subtitle)* SENSITIVITY ANALYSIS FOR PREMIXED, LAMINAR, STEADY-STATE FLAMES		5. TYPE OF REPORT & PERIOD COVERED 6. PERFORMING ORG. REPORT NUMBER
7. AUTHOR*(s)* T.P. COFFEE AND J.M. HEIMERL		8. CONTRACT OR GRANT NUMBER*(s)*
9. PERFORMING ORGANIZATION NAME AND ADDRESS U.S. Army Ballistic Research Laboratory ATTN: DRDAR-BLI Aberdeen Proving Ground, MD 21005		10. PROGRAM ELEMENT, PROJECT, TASK AREA & WORK UNIT NUMBERS 1L162618AH80
11. CONTROLLING OFFICE NAME AND ADDRESS US Army Armament Research & Development Command US Army Ballistic Research Laboratory (DRDAR-BL) Aberdeen Proving Ground, MD 21005		12. REPORT DATE January 1983 13. NUMBER OF PAGES 67
14. MONITORING AGENCY NAME & ADDRESS*(if different from Controlling Office)*		15. SECURITY CLASS. *(of this report)* UNCLASSIFIED 15a. DECLASSIFICATION/DOWNGRADING SCHEDULE

16. DISTRIBUTION STATEMENT *(of this Report)*

Approved for public release; distribution unlimited

17. DISTRIBUTION STATEMENT *(of the abstract entered in Block 20, if different from Report)*

18. SUPPLEMENTARY NOTES

19. KEY WORDS *(Continue on reverse side if necessary and identify by block number)*

Laminar Flames
Premixed Flames
Steady-State Flames
One Dimensional Flames
Sensitivity Analysis

20. ABSTRACT *(Continue on reverse side if necessary and identify by block number)*

raj

A procedure has been developed to perform a sensitivity analysis on the transport and rate input parameters for a premixed, laminar, one-dimensional, steady-state flame. Computer codes exist to perform the sensitivity analysis automatically. The analysis can be done in terms of Taylor expansions or Logarithmic expansions. Both first and second order coefficients may be computed.

DD FORM 1 JAN 73 1473 EDITION OF 1 NOV 65 IS OBSOLETE

UNCLASSIFIED

SECURITY CLASSIFICATION OF THIS PAGE *(When Date Entered)*

Abstract (Cont'd):

20. As a test case, the analysis has been carried out for a set of $H_2/O_2/N_2$/flames. The relative accuracy and the range of validity of the various expansions is discussed.

TABLE OF CONTENTS

LIST OF TABLES

LIST OF FIGURES

LIST OF FIGURES (cont'd)

FIGURE PAGE

I. INTRODUCTION

We are interested in determining validated sets of elementary chemical reactions for use in predictive combustion models. The approach used has been to simulate the one dimensional, premixed, laminar steady-state flame. This approach has the advantage that the predicted temperature and species profiles, as well as the flame speeds, can in principle be compared with suitable burner experiments of the flame.

Such a model requires as input data sets of (1) thermodynamic coefficients, (2) transport coefficients, and (3) chemical reactions, including their rate coefficients. Often, many of the input parameters, and in particular the rate coefficients, are not well known. Therefore, it is useful to be able to perform a sensitivity analysis, so as to systematically determine the effect of uncertain parameters on the solutions of the model. If the system is very sensitive to a given parameter, more time and effort may be justified to determine a more accurate value for that parameter. On the other hand, an insensitive parameter requires less effort; and it may be possible to eliminate it and thus simplify a complex system. In addition, the sensitivity analysis is useful in understanding a complex mechanism, since it indicates which parts of the mechanism are important for a given problem.

We are also interested in the region of applicability of our sensitivity analysis. Since some of our input parameters have wide limits of uncertainty, the sensitivity of the system may change considerably as our parameter value is changed. It is therefore useful to have some idea of the region in which the sensitivity analysis is valid.

In this paper the results are given for a sensitivity analysis performed on a set of $H_2 - O_2 - N_2$ flames. The input parameters considered variable are the transport coefficients and the rate coefficients. Since the thermodynamic properties for this flame are well known, our sensitivity analysis has not been extended to cover these input parameters. Similarly, because the ratio between the forward and the backward rate coefficients of a reaction is determined by the thermodynamic properties, the effect of varying this ratio is not considered either. The appendix outlines the sources of input parameters used.

Section II gives the governing equations, both for the basic model and for the sensitivity coefficients. Section III reports the results for the two special cases that can be solved analytically. In Section IV, we discuss a numerical procedure. Section V gives the numerical results for our test set of flames. In Sections VI and VII we develop the second order sensitivity analysis, and in Section VIII we discuss the accuracy of extrapolating the results when the parameters vary over a large range.

II. GOVERNING EQUATIONS

We are interested in the equations that describe a one-dimensional, laminar, premixed flame propagating in an unbounded ideal gas. Since performing the sensitivity analysis numerically is expensive, it is useful to simplify the equations as much as possible. A high degree of accuracy is not required, since we are interested in trends.

In a previous paper[1], we considered various levels of approximation to the multicomponent transport coefficients. A relatively simple approximation (Method V), gave very accurate results and will be used here. The corresponding equations are the following.

Continuity for species 1 through N-1 is expressed in the form

$$\frac{\partial Y_i}{\partial t} + m_o \frac{\partial Y_i}{\partial \psi} = \rho^2 D_{im} \frac{\partial^2 Y_i}{\partial \psi^2} + \frac{R_i M_i}{\rho} \quad i = 1, \ldots, N-1, \qquad (1)$$

and continuity of the Nth species in the form

$$Y_N = 1 - \sum_{i=1}^{N-1} Y_i \ . \qquad (2)$$

Here t is the time, Y_i the mass fraction of the ith species, m_o the mass flux through the cold boundary; ψ a transformed space coordinate, ρ the density of the mixture, D_{im} the diffusion coefficient of the ith species into the mixture, M_i the molecular weight of species i and R_i the net rate of production of species i due to chemical reactions. The ψ coordinate is related to the spatial coodinate x by

$$\psi = \int_o^x \rho\,(x')\, dx' \ . \qquad (3)$$

Conservation of energy is expressed by

$$\frac{\partial T}{\partial t} + m_o \frac{\partial T}{\partial \psi} = \frac{\rho\lambda}{c_p} \frac{\partial^2 T}{\partial \psi^2} - \frac{1}{\rho c_p} \sum_{i=1}^{N} R_i M_i h_i , \qquad (4)$$

where T is the temperature of the mixture, λ the thermal conductivity of the mixture, c_p the specific heat of the mixture and h_i the specific enthalpy of species i, given by

$$h_i = h_i^o + c_p\,(T - T_o) \ , \qquad (5)$$

where T_o is a fixed reference temperature and h_i^o is the enthalpy at that temperature. The boundary conditions are

$$T = T_u \quad \text{and} \quad Y_i = Y_{iu} \ , \quad i = 1,2, \ldots N-1 \qquad (6)$$

---

[1] *T.P. Coffee and J.M. Heimerl, "Transport Algorithms for Premixed, Laminar Steady State Flames," Combustion and Flame, Vol. 43, pp. 273-289, 1981.*

at $x = \psi = -\infty$ and

$$\frac{\partial T}{\partial \psi} = \frac{\partial Y_i}{\partial \psi} = 0, \quad i = 1,2,\ldots N-1 \tag{7}$$

at $x = \psi = +\infty$. The above system of equations is closed by relations that express the production rates R_i in terms of the temperature, mass fractions, and a set of chemical parameters.

In the above equations, the effects of radiation, viscosity, and body forces are ignored. Since the burning velocity is small compared with the local speed of sound, the pressure is taken to be constant. Besides these standard assumptions, we have also assumed that the thermal diffusion is negligibly small, that Fick's law holds for the diffusion velocities, and that the quantities $\rho^2 D_{im}$, $\rho\lambda$, and c_p are constant. These constants are chosen a priori.[1]

Our interest is in the steady state solution. The numerical procedure is to start with arbitrary profiles $Y_i(\psi)$ and $T(\psi)$ and integrate in time until the steady state solution is achieved. As the integration proceeds, the mass flux m_o through the origin is iteratively adjusted to equal the mass flux through the flame, so that at steady state the flame is motionless with respect to the coordinate system used. The burning velocity, S, of the flame is defined as the velocity of the flame relative to the fluid at rest, i.e., at $x = -\infty$. Since in our coordinate system the flame is at rest, $S = v(-\infty) = m_o/\rho_u$, where ρ_u is the density of the unburned mixture.

The solution of the Eqs. (1) through (7) establishes benchmark values of the burning velocity and the temperature and species profiles for a given set of input parameters. Details of the numerical procedure are in References 2 and 3.

The production rate functions, $R_i(T)$, are defined by

$$R_i = \sum_{r=1}^{NR} R_{ir} = \sum_{r=1}^{NR} (v''_{i,r} - v'_{i,r}) \left[k_{fr} \prod_{j=1}^{N} (C_j)^{v'_{j,r}} - k_{br} \prod_{j=1}^{N} (C_j)^{v''_{j,r}}\right] \tag{8}$$

where $v''_{i,r}$ and $v'_{i,r}$ are the number of molecules of species i entering into reaction r as product and reactant, respectively, C_j is the concentration of the jth species and k_{fr} and k_{br} are the forward and reverse rate coefficients, respectively. The rate coefficients depend on the temperature through the

---

[2] *T.P. Coffee and J.M. Heimerl, "A Method for Computing the Flame Speed for a Laminar, Premixed, One Dimensional Flame," BRL Technical Report, ARBRL-TR-02212, Jan. 1980, (AD#A082803).*

[3] *T.P. Coffee, "A Computer Code for the Solution of the Equations Governing a Laminar, Premixed, One Dimensional Flame," BRL Memorandum Report, ARBRL-MR-03165, April 1982, (AD#A114041).*

Arrhenius relations

$$k_{fr} = A_{fr}\, T^{B_{fr}} \exp(-E_{fr}/RT)$$

and

$$k_{br} = A_{br}\, T^{B_{br}} \exp(-E_{br}/RT), \qquad (9)$$

where R is the gas constant, E is the activation energy and A is the frequency factor for the reaction. In Eq. (9) the parameters B_{fr}, B_{br}, E_{fr} and E_{br} will be held constant and sensitivity analysis will be restricted to variations in A_{fr}. Since thermodynamic quantities are held constant the ratio A_{fr}/A_{br} is also constant. We will also investigate the effects of variations of the parameters $\rho^2 D_{im}$, i = 1, ..., N - 1 and $\rho\lambda$ in Eqs. (1) and (4). The remaining parameters c_p, M_i and h_i^o are held fixed. Thus we have a total of NT = N + NR variable parameters. See Table 1.

TABLE 1. PARAMETERS DEFINING THE FLAME.

Parameter	Constant	Variable
Mixture	c_p	$\rho\lambda \times \alpha_{NT}$
Species (i = 1, ..., N)	h_i^o, M_i	$\rho^2 D_{im} \times \alpha_{NR+i}$
Reaction	E_{fr}, B_{fr}	$A_{fr} \times \alpha_r$
(r=1,...,NR)	E_{br}, B_{br}	$A_{br} \times \alpha_r$

The variation is expressed by attaching factors α_i, i = 1, ..., NT to the benchmark values of the variable parameters. Then Eqs. (1) and (4) become

$$\frac{\partial Y_i}{\partial t} + m_o \frac{\partial Y_i}{\partial \psi} = \alpha_{NR+i} \rho^2 D_{im} \frac{\partial^2 Y_i}{\partial \psi^2} + \sum_{r=1}^{NR} \alpha_r R_{ir} M_i/\rho, \quad i=1,2\ldots,N-1 \qquad (10)$$

and

$$\frac{\partial T}{\partial t} + m_o \frac{\partial T}{\partial \psi} = \frac{\alpha_{NT}\, \rho\lambda}{c_p} \frac{\partial^2 T}{\partial \psi^2} - \frac{1}{c_p} \sum_{i=1}^{N} \sum_{r=1}^{NR} \alpha_r R_{ir} M_i h_i . \qquad (11)$$

When $\alpha_1 = \ldots = \alpha_{NT} = 1$, Eqs. (10) and (11) are just the benchmark Eqs. (1) and (4). Changes in α_i (i=1, ... NR) correspond to changes in the rate coefficients k_{fi} and k_{bi}; changes in α_i (i = NR+1, ... NT) correspond to changes in the transport coefficients $\rho^2 D_{im}$ and $\rho\lambda$. The basic problem is to determine how changes in the α_i affect the output functions S, Y_i and T.

III. ANALYTIC RESULTS

Two special cases can be solved analytically. Consider the case $\alpha_1 = \ldots \alpha_{NR} = 1$, $\alpha_{NR+1} = \ldots = \alpha_{NT} = \alpha$ Then Eqs. (10) and (11) can be written

$$\frac{\partial Y_i}{\partial t} + m_o \frac{\partial Y_i}{\partial \psi} = \alpha \rho^2 D_{im} \frac{\partial^2 Y_i}{\partial \psi^2} + \frac{R_i M_i}{\rho} \tag{12}$$

and

$$\frac{\partial T}{\partial t} + m_o \frac{\partial T}{\partial \psi} = \frac{\alpha \rho \lambda}{c_p} \frac{\partial^2 T}{\partial \psi^2} - \frac{1}{\rho c_p} \sum_{i=1}^{N} R_i M_i h_i . \tag{13}$$

Apply the coordinate transformation $\psi' = \psi/\sqrt{\alpha}$. Then the above equations become:

$$\frac{\partial Y_i}{\partial t} + \frac{m_o}{\sqrt{\alpha}} \frac{\partial Y_i}{\partial \psi'} = \rho^2 D_{im} \frac{\partial^2 Y_i}{\partial \psi'^2} + \frac{R_i M_i}{\rho} \tag{14}$$

and

$$\frac{\partial T}{\partial t} + \frac{m_o}{\sqrt{\alpha}} \frac{\partial T}{\partial \psi'} = \frac{\rho \lambda}{c_p} \frac{\partial^2 T}{\partial \psi'^2} - \frac{1}{\rho c_p} \sum_{i=1}^{N} R_i M_i h_i . \tag{15}$$

Eqs. (14) and (15) are formally identical to the benchmark Eqs. (1) and (4) except that the mass flux factor m_o in these equations is replaced by $m_o/\sqrt{\alpha}$. Thus, multiplying all the transport coefficients by a uniform factor α causes the mass flux (and hence the burning velocity) to change by a factor $\sqrt{\alpha}$. Similarly, the profiles in ψ' space are identical to the benchmark profiles in ψ space. That is, the profiles are expanded ($\alpha > 1$) or contracted ($\alpha < 1$) uniformly by a factor $\sqrt{\alpha}$ in the original ψ space. This fact has been noted by Dixon-Lewis[4].

A similar result follows if all the rate coeffients are multiplied by a uniform factor α, that is, $\alpha_1 = \ldots \alpha_{NR} = \alpha, \alpha_{NR+1} = \ldots = \alpha_{NT} = 1$. Then using the coordinate transformation $\psi' = \psi\sqrt{\alpha}$ and dividing by α, one obtains

$$\frac{1}{\alpha} \frac{\partial Y_i}{\partial t} + \frac{m_o}{\sqrt{\alpha}} \frac{\partial Y_i}{\partial \psi'} = \rho^2 D_{im} \frac{\partial^2 Y_i}{\partial \psi'^2} + \frac{R_i M_i}{\rho} \tag{16}$$

---

[4] *G. Dixon-Lewis, "Flame Structure and Flame Reaction Kinetics. I. Solution of Conservation Equations and Application to Rich Hydrogen-Oxygen Flames," Proc. Roy. Soc., London A, Vol. 298, pp. 495-513, 1967.*

and

$$\frac{1}{\alpha}\frac{\partial T}{\partial t} + \frac{m_o}{\sqrt{\alpha}}\frac{\partial T}{\partial \psi'} = \frac{\rho\lambda}{c_p}\frac{\partial^2 T}{\partial \psi'^2} - \frac{1}{\rho c_p}\sum_{i=1}^{N} R_i M_i h_i \quad . \qquad (17)$$

For the steady state solution, multiplying all the rates by a uniform factor α causes the burning velocity to change by a factor $\sqrt{\alpha}$ while the profiles are contracted ($\alpha > 1$) or expanded ($\alpha < 1$) in the same proportion.

So the overall effect of increasing the transport coefficients is to spread the flame front, as energy and species diffuse more rapidly away from the flame front. The effect of increasing all the rates is to contract the flame front, as the overall combustion occurs more rapidly.

These effects are independent. That is, if all the transport coefficients and all the rate coefficients are multiplied by the same factor α, then the flame speed S will change by a factor α, while the species and temperature profiles will be identical with the solutions of the benchmark equations.

IV. NUMERICAL PROCEDURES

Several approaches have been used to perform sensitivity analyses, mostly for systems of ordinary differential equations in time. These are either local (valid for input parameters near the benchmark values) or global (valid over a specified range). Since some rate coefficients have large regions of uncertainty, a global procedure would be preferred. The simplest procedure is to solve the equations for different values of the input parameters over their range of uncertainty. For large numbers of parameters whose regions of uncertainty are also large, this simple procedure is inefficient. A more efficient procedure has been devised by Shuler and coworkers[5-7], the Fourier Amplitude Sensitivity Test (FAST). In this procedure the input parameters are varied simultaneously, and the results are Fourier analyzed. However, as the number of input parameters increases, the number of computations required increases rapidly and the cost for our system of PDE's is still prohibitive.

Therefore we use a local method based on a Taylor series expansion with respect to variations of the parameters α_j. We introduce the notation

---

[5] *R.I. Cukier, C.M., Fortuin, K.E. Shuler, A.G. Petschek, and J.H. Schaibley, "Study of the Sensitivity of Coupled Reaction Systems to Uncertainties in Rate Coefficients I. Theory," J. Chem. Phys., Vol. 59, pp. 3873-3878, 1973.*

[6] *J.H. Schaibly and K.E. Shuler, "Study of the Sensitivity of Coupled Reaction Systems to Uncertainties in Rate Coefficients II. Applications," J. Chem. Phys., Vol. 59, pp. 3879-3888, 1973.*

[7] *R.I. Cukier, J.H. Schaibly, and K.E. Shuler, "Study of the Sensitivity of Coupled Reaction Systems to Uncertainties in Rate Coefficients III. Analysis of the Approximations," J. Chem. Phys., Vol. 63, pp. 1140-1149, 1975.*

$F^j \equiv \partial F/\partial \alpha_j$ evaluated $\alpha_1 = \ldots = \alpha_{NT} = 1$ (F = S, Y_i or T). We expand the flame speed, S, to first order and find

$$S_N \tilde{-} S_B + \sum_{j=1}^{NT} S^j \ (\alpha_j - 1), \tag{18}$$

where S_B is the benchmark flame speed and S_N is the flame speed for other choices of the α_j. Similar expansions are used for Y_i and T.

The partial derivatives S^j, $Y_i{}^j$ and T^j, i.e. the "sensitivity coefficients", are computed numerically. To that end we take the partial derivatives of Eqs. (10) and (11) with respect to α_j and let the α's approach one. The resulting equations are

$$\frac{\partial Y_i{}^j}{\partial t} + m_o{}^j \frac{\partial Y_i^j}{\partial \psi} + m_o \frac{\partial Y_i{}^j}{\partial \psi} = \delta_{NR+i,j} \rho^2 D_{im} \frac{\partial^2 Y_i}{\partial \psi^2} + \rho^2 D_{im} \frac{\partial^2 Y_i{}^j}{\partial \psi^2} +$$

$$\sum_{r=1}^{NR} \left[\delta_{r,j} \frac{R_{ir} M_i}{\rho} + \left(\frac{M_i R_{ir}}{\rho}\right)^j\right] \tag{19}$$

and

$$\frac{\partial T^j}{\partial t} + m_o{}^j \frac{\partial T}{\partial \psi} + m_o \frac{\partial T^j}{\partial \psi} = \delta_{NT,j} \frac{\rho\lambda}{c_p} \frac{\partial^2 T}{\partial \psi^2} + \frac{\rho\lambda}{c_p} \frac{\partial^2 T^j}{\partial \psi^2} -$$

$$\frac{1}{c_p} \sum_{i=1}^{N} \sum_{r=1}^{NR} \left[\frac{\delta_{r,j} R_{ir} M_i h_i}{\rho} + \frac{R_{ir} M_i h_i{}^j}{\rho} + \left(\frac{R_{ir} M_i}{\rho}\right)^j h_i\right], \tag{20}$$

where from Eq. (5) we see that $h_i{}^j = c_p T^j$. Introduction of the notation

$$u_i = Y_i, \ i = 1, \ldots N, \tag{21}$$

$$\text{and } u_{N+1} = T,$$

allows us to write the identity

$$\left(\frac{R_{ir} M_i}{\rho}\right)^j = \sum_{m=1}^{N+1} \left[\partial \left(\frac{R_{ir} M_i}{\rho}\right)/\partial u_m\right] u_m{}^j . \tag{22}$$

Equations (19) through (22) constitute a system of differential equations for the functions $u_m{}^j$. This system is similar to that given by Eqs. (1) through (7) and is solved using the same numerical relaxation technique outlined in Section II.

This numerical solution is called the Direct Method and is accomplished as follows. First the benchmark Eqs. (1) and (4) are solved. The benchmark values for m_o, the values for the species and temperature, and their first and second derivatives are stored in a file. (We use a finite element code in

which the solutions are represented by piecewise polynomials. Therefore the derivatives are available. Also the code uses a collocation method so that only the values at the collocation points need to be saved.) The terms $(R_{ir}M_i/\rho)$ and $\partial(R_{ir}M_i/\rho)/\partial u_m$ are computed in subroutines and the benchmark values of these expressions are also saved. Finally, Eqs. (19) and (20) are solved for each selected set of α_j, providing us with the corresponding set of m_o^j and u_i^j .

Another method for finding the linear sensitivity coefficients is the Green's function method.[8] For ordinary differential equations this involves solving a set of N equations to determine the Green's functions, instead of a set of NT equations. Then the sensitivity coefficients are found by a set of quadratures. Higher order sensitivity coefficients can also be determined by the same method.

In a recent paper[9], the theory was extended to partial differential equations. In that case the Green's functions are represented as a linear combination of independent solutions of the homogeneous equations based on our Eqs. (19) and (20). Each independent solution is found by solving the homogeneous equations with a different set of boundary conditions. We implemented this procedure, but the solutions obtained were not numerically independent. This is due to the fact that the steady state solutions of the flame equations are almost independent of the downstream (or hot) boundary conditions. So this procedure cannot be used for the steady state flame equations.

Once the sensitivity coefficients have been obtained, the usual way to determine the values of the output functions that correspond to changes in the input parameters is by the linear terms of a Taylor series, such as Eq. (18). However, the results of Section III indicate that at least for two special cases, the extrapolation $S_N = S_B\,\alpha^{.5}$ is exact. This suggests that a better approximation than Eq. (18) may be the formula

$$S_N \tilde{=} S_B \prod_{j=1}^{NT} \alpha_j^{S_E^j} . \qquad (23)$$

where the S_E^j are appropriate sensitivity exponents. Taking logarithms, Eq. (23) becomes

---

[8] *J.T. Hwang, E.P. Dougherty, S. Rabitz and H. Rabitz, "The Green's Function Method of Sensitivity Analysis in Chemical Kinetics,"* J. Chem. Phys., *Vol. 69, pp. 5180-5191, 1978.*

[9] *M. Demiralp and H. Rabitz, "Chemical Kinetic Functional Sensitivity Analysis: Elementary Sensitivities,"* J. Chem. Phys., *Vol. 74, pp. 3362-3375. 1981.*

$$\ln S_N \tilde{=} \ln S_B + \sum_{j=1}^{NT} S_E^j \ln\alpha_j . \qquad (24)$$

Eq. (24) represents the linear Taylor expansion of $\ln (S_N)$ in terms of $\ln \alpha_j$. This form permits some checks on the numerical solution. Eq. (23) becomes exact as the α_j's approach one. But if we consider the case where $\alpha_1 = \ldots = \alpha_{NR}$ or $\alpha_{NR+1} = \ldots = \alpha_{NT}$, then $S_N = S_B^{0.5}$. Equating exponents, we find

$$\sum_{j=1}^{NR} S_E^j = \sum_{j=NR+1}^{NT} S_E^j = 0.5, \qquad (25)$$

The corresponding relation for the profile sensitivity coefficients is

$$\sum_{j=1}^{NT} u_{iE}^j = 0 \qquad (26)$$

for any value of ψ.

The relation between the sensitivity coefficients S^j and S_E^j is straightforward. Taking the derivative of Eq. (24) with respect to α_m results in

$$\frac{1}{S_N} \frac{\partial S_N}{\partial \alpha_m} \tilde{=} S_E^m \frac{1}{\alpha_m} , \qquad (27)$$

and in the limit $\alpha_m \to 1$,

$$S_E^m = S^m / S_B . \qquad (28)$$

The corresponding formula for the u_{iE}^j is

$$u_{iE}^j = u_i^j / u_{iB} . \qquad (29)$$

The logarithmic sensitivity form (24) has been used before[10]. In particular, it has been recommended for the modelling of chemical reactions without transport, where logarithmic measures of species concentrations as a

---

[10] P.M. Frank, "Introduction to System Sensitivity Theory," Academic Press, 1978.

function of time are appropriate[11]. We will show that it is also useful for steady state flames.

V. NUMERICAL RESULTS AND DISCUSSION

The above procedure was carried out for a set of four $H_2 - O_2 - N_2$ flames. The chemistry scheme used is due to Dixon-Lewis[12] and consists of eight species and seventeen reactions. The input parameters are given in Appendix A.

The initial mole fractions and temperature for the flames are given in Table 2. The benchmark flame speeds are also given. These values are slightly different from the flame speeds calculated using a more accurate transport algorithm. The total pressure is fixed at one atmosphere for all the flames.

Flame A is a very fast, stoichiometric flame. Flame B is a hydrogen rich flame with a more moderate flame speed. Flame C is an oxygen rich flame. The initial mole fractions were chosen so that the flame speed is similar to that of flame B. Flame D is a very slow, hydrogen rich flame. This flame has been studied extensively by Dixon-Lewis[13].

TABLE 2. MOLE FRACTIONS, INITIAL TEMPERATURE AND BENCHMARK FLAME SPEEDS FOR THE FOUR FLAMES STUDIED.

FLAME	X_{H2}	X_{O2}	X_{N2}	T_U(K)	S_B(cm-s^{-1})
A	.6667	.3333	.0000	298	858.0
B	.5000	.1050	.3950	298	251.9
C	.3000	.5600	.1400	298	285.7
D	.1883	.0460	.7657	336	11.8

[11] *W.C. Gardiner, Jr., "The pC, pR, pP, pM, and pS Method of Formulating the Results of Computer Modeling Studies of Chemical Reactions,"* J. Phys. Chem., *Vol . 81, pp. 2367-2371, 1977.*

[12] *G. Dixon-Lewis, "Kinetic Mechanism, Structure and Properties of Premixed Flames in Hydrogen-Oxygen-Nitrogen Mixtures,"* Proc. R. Soc. London A, *Vol. 292, pp. 45-99, 1979.*

[13] *G. Dixon-Lewis, M.M. Sutton, and A. Williams, "Flame Structure and Flame Reaction Kinetics IV. Experimental Investigations of a Fuel-Rich Hydrogen + Oxygen + Nitrogen Flame at Atmospheric Pressure,"* Proc. Roy. Soc. London A., *Vol. 312, pp. 227-234, 1970.*

Table 3 gives the sensitivity exponents S_E^j of the transport parameters and Table 4 gives them for the rate coefficients. Where possible we have taken the Nth species of Eq. (2) to be the diluent, N_2. Thus, for flames B, C and D an entry for $\rho^2 D_{N_m}$ does not appear. (See Table 1). Since flame A has no diluent and is described by one less species, we have taken the Nth species to be H_2O. Consequently, no entry appears in Table 3 for H_2O, flame A. Likewise in Table 4 reaction 12 is zero and no entry appears.

Comparing the $\Sigma\ S_E^j$ from the numerical values of Tables 3 and 4 with the analytic result given by Eq. (25), we find excellant agreement.

The tables also give the sum of the absolute values of the S_E^j. We will refer to this number as the overall sensitivity (for transport or chemistry). It will be shown that this number provides a rough estimate of the complexity of the flame and its sensitivity to changes in the input parameters.

Consider first the transport parameters. A flame front can propagate by two processes: diffusion of radicals (H, OH, O, HO_2) ahead of the flame or conduction of heat ahead of the flame. Among the radicals, the flames are most sensitive to the diffusion of H. This is reasonable since H is light and diffuses easily. The faster flames are more sensitive to the diffusion of

TABLE 3. FLAME SPEED SENSITIVITY EXPONENTS, S_E^j, FOR THE TRANSPORT PARAMETERS.

Parameter		A	B	C	D
$\rho^2 D_{1m}$	H	.3545	.3785	.2018	.0123
$\rho^2 D_{2m}$	OH	.0250	.0012	.0647	-.0013
$\rho^2 D_{3m}$	O	.0339	-.0011	.0936	-.0033
$\rho^2 D_{4m}$	HO_2	.0001	-.0000	-.0008	.0001
$\rho^2 D_{5m}$	H_2	-.0069	.0079	-.2689	-.0025
$\rho^2 D_{6m}$	O_2	-.0237	-.1207	-.0159	-.4176
$\rho^2 D_{7m}$	H_2O	*	.0162	.0232	-.0406
$\rho\lambda$		.1179	.2191	.4039	.9521
$\sum_{j=NR+1}^{NT} S_E^j$		.5009	.5010	.5017	.4992
$\sum_{j=NR+1}^{NT} \lvert S_E^j \rvert$		.5620	.7446	1.0727	1.4298

*no entry, see text.

TABLE 4. FLAME SPEED SENSITIVITY EXPONENTS, S_E^j, FOR THE RATE COEFFICIENTS

Rate Coefficient	Reaction	A	B	C	D
1	$OH+H_2 \rightarrow H_2O+H$	.1346	.0744	.3140	.0576
2	$H+O_2 \rightarrow OH+O$	.1041	.2911	.0400	1.2427
3	$O+H_2 \rightarrow OH+H$	.0907	.0468	.1718	.0347
4	$H+O_2+M' \rightarrow HO_2+M'$	.1879	.1838	.0301	-.5312
5	$H+HO_2 \rightarrow OH+OH$	.0503	.1099	.0997	.7492
6	$H+HO_2 \rightarrow O+H_2O$	-.0053	-.0054	-.0111	.0389
7	$H+HO_2 \rightarrow H_2+O_2$	-.0399	-.0952	-.0666	-.7555
8	$OH+HO_2 \rightarrow H_2O+O_2$	-.0056	-.0092	-.0208	-.0187
9	$O+HO_2 \rightarrow OH+O_2$	-.0005	-.0011	-.0006	-.0125
10	$O+HO_2 \rightarrow OH+O_2$	-.0001	-.0002	-.0000	-.0022
11	$H+H+H_2 \rightarrow H_2+H_2$	-.0003	-.0142	-.0002	-.0222
12	$H+H+N_2 \rightarrow H_2+N_2$	*	-.0111	-.0001	-.1146
13	$H+H+O_2 \rightarrow H_2+O_2$	-.0001	-.0009	-.0005	-.0007
14	$H+H+H_2O \rightarrow H_2+H_2O$	-.0014	-.0419	-.0014	-.1339
15	$H+OH+M'' \rightarrow H_2O+M''$	-.0047	-.0213	-.0112	-.0296
16	$H+O+M'' \rightarrow OH+M''$	.0001	-.0007	-.0008	-.0015
17	$OH+OH \rightarrow O+H_2O$	-.0106	-.0060	-.0440	.0001
$\sum_{j=1}^{NR} S_E^j$		.4991	.4990	.4983	.5008
$\sum_{j=1}^{NR} \lvert S_E^j \rvert$		.6362	.9131	.8128	3.7458

* no entry, see text.

radicals, since their flame fronts have larger radical concentrations and steeper gradients than the slower flames. Increasing the thermal conductivity increases the flame speed. This effect progressively becomes more important the slower the flame because diffusion becomes less important.

The diffusion of H_2 and O_2 tends to slow down the flame, since they tend to diffuse away from the flame front. The hydrogen rich flames, B and D, are sensitive to the diffusion of oxygen since oxygen is in short supply, while the oxygen rich flame, C, is sensitive to the diffusion of hydrogen.

The results for the chemistry are consistent with the prevailing view of the mechanism. Most of the product H_2O is created by reaction 1 [$OH+H_2 \rightarrow H_2O+H$] and increases in this rate will increase the flame speed. Note that flame C is especially sensitive to this rate. Since flame C is deficient in H_2, reaction 1 is slower relative to the other flames. A slower reaction can be a bottleneck for an entire process with the consequence that a flame can become quite sensitive to changes in the bottleneck reaction rate.

The OH required in reaction 1 is primarily produced by the chain-branching reactions 2 [$H+O_2 \rightarrow OH+O$] and 3 [$O+H_2 \rightarrow OH+H$]. The hydrogen rich flames B and D are more sensitive to reaction 2 (shortage of O_2) and the oxygen rich flame C is more sensitive to reaction 3 (shortage of H_2). For the stoichiometric flame A, the sensitivities are comparable.

OH can also be created by the reaction pathway 4[$H+O_2+M \rightarrow HO_2+M$] and 5[$H+HO_2 \rightarrow OH+OH$]. Reaction 5 is in competition with reaction 7[$H+HO_2 \rightarrow H_2+O_2$]. For flames A,B, and C, increasing rate coefficients 4 and 5 will increase the flame speed, while increasing rate coefficient 7 will decrease the flame speed. The other reactions are relatively unimportant for these flames.

Because of the fact that the concentration of H is very small, flame D exhibits a different behavior. If rate coefficient 4 is increased, the flame speed decreases. That is, the shortage of H is aggravated, which slows down the total network. For the same reason, flame D is very sensitive to the recombination reactions (11,12, and 14).

Flame D is in fact very close to the point of extinction. A relatively small change in an input parameter (increasing rate coefficients 4 or 7; decreasing rate coefficients 2 or 5) can extinguish the flame. Conversely, a relatively small change in the opposite direction can lead to a large increase in the flame speed. This complex balance between several competing reactions is reflected in the fact that the overall sensitivity $\sum_{j=1}^{NR} |S_E^j|$ is large.

We are also interested in the sensitivity of the species and temperature profiles. In this case there are some problems in presenting the results in terms of the sensitivity exponents given by Eq. (29). Near the upstream (or cold) boundary, some of the mass fractions u_{iB} approach zero. Thus in this region small numerical errors in either u_i^j or u_{iB} lead to large errors in u_{iE}^j. As a heuristic correction we set $u_{iE}^j = 0$ if $u_{iB} < u_{iB}(\max) \times 10^{-3}$ where

$u_{iB}(max)$ is the maximum value of the benchmark profile. Another difficulty occurs just ahead of the flame front. Our analytic results indicate that a flame front may expand due to changes in the input parameters. In that case, a small value of u_{iB} just ahead of the flame front can correspond to a relatively large sensitivity coefficient u_i^j, and therefore the u_{iE}^j is large. This large value can determine the scale of a plot of the logarithmic sensitivity profiles, with the result that the details of these profiles in the region of the flame front may be lost. Therefore, it is more practical to graph the sensitivity coefficients u_i^j rather than the u_{iE}^j. For ease of comparison, we normalize the profiles by dividing the u_i^j by the $u_{iB}(max)$. (All calculations are carried out in ψ - space and , for easier interpretation, are converted to x-space before graphing.)

Figures 1 and 2 show the benchmark mass fraction profiles for OH (radical) and H_2 (major species), respectively. We have taken these two species and flame B as representative examples. The normalized sensitivity coefficients profiles for $\rho^2 D_H$, $\rho^2 D_{H2}$, $\rho^2 D_{O2}$ and $\rho\lambda$ are given in Figures 3 and 4. The profiles for reaction rate coefficients 1,2,4,5, and 7 are shown in Figures 5 and 6. All other transport and rate coefficient sensitivity profiles for flame B are small. The profiles for OH are larger, because of the normalization. A small relative change in a major species concentration can lead to large relative changes in the radical concentrations, because the radical concentrations are much smaller.

In general the diffusion of H is the most important transport parameter. The sensitivity coefficients in Figure 3 show that increasing $\rho^2 D_H$ leads to a sharp increase of the first OH bump in the early part of the flame of Figure 1. We see in Figure 4 that the diffusion of H_2 is important in determining the H_2 profile, but it has a minor effect on all the other profiles.

The chemistry profiles are more complicated, since different reactions can be important at different locations in the flame front. In Figures 5 and 6 we see that rate coefficient 2 ($H+H_2 \rightarrow OH+O$) is the most important. The complicated appearance of the sensitivity coefficients for the OH profiles in Figure 5 is due to competition between the chain branching rates and the HO_2 rates in the early part of the flame front.

The results for flame C (not shown) are similar to those given above, except that rate coefficient 3($O+H_2 \rightarrow OH+H$) becomes important.

For the fast flame A, the radical concentrations are almost as large as the major species concentrations ($Y_{OH}^{(max)} = .1104$; $Y_{H2}^{(max)} = .1111$). As a result, the normalized OH sensitivity coefficients are about the same size as the H_2 coefficients. The profiles are relatively insensitive to changes in the input parameters. In general, the same set of input parameters as before are important for flame A. The exception is in the post flame region where, because of the large radical concentrations, rate coefficients 13 and 14 become important.

For the slow flame D, the radical concentrations are very small ($Y_{OH}^{(max)} = 1.09 \times 10^{-5}$), so that the normalized sensitivity coefficients are quite large (on the order of 1.0 for transport, 2.0 for chemistry). The same input parameters as for flame B are important; except that, because of the low concentration of H, the diffusion of H is unimportant.

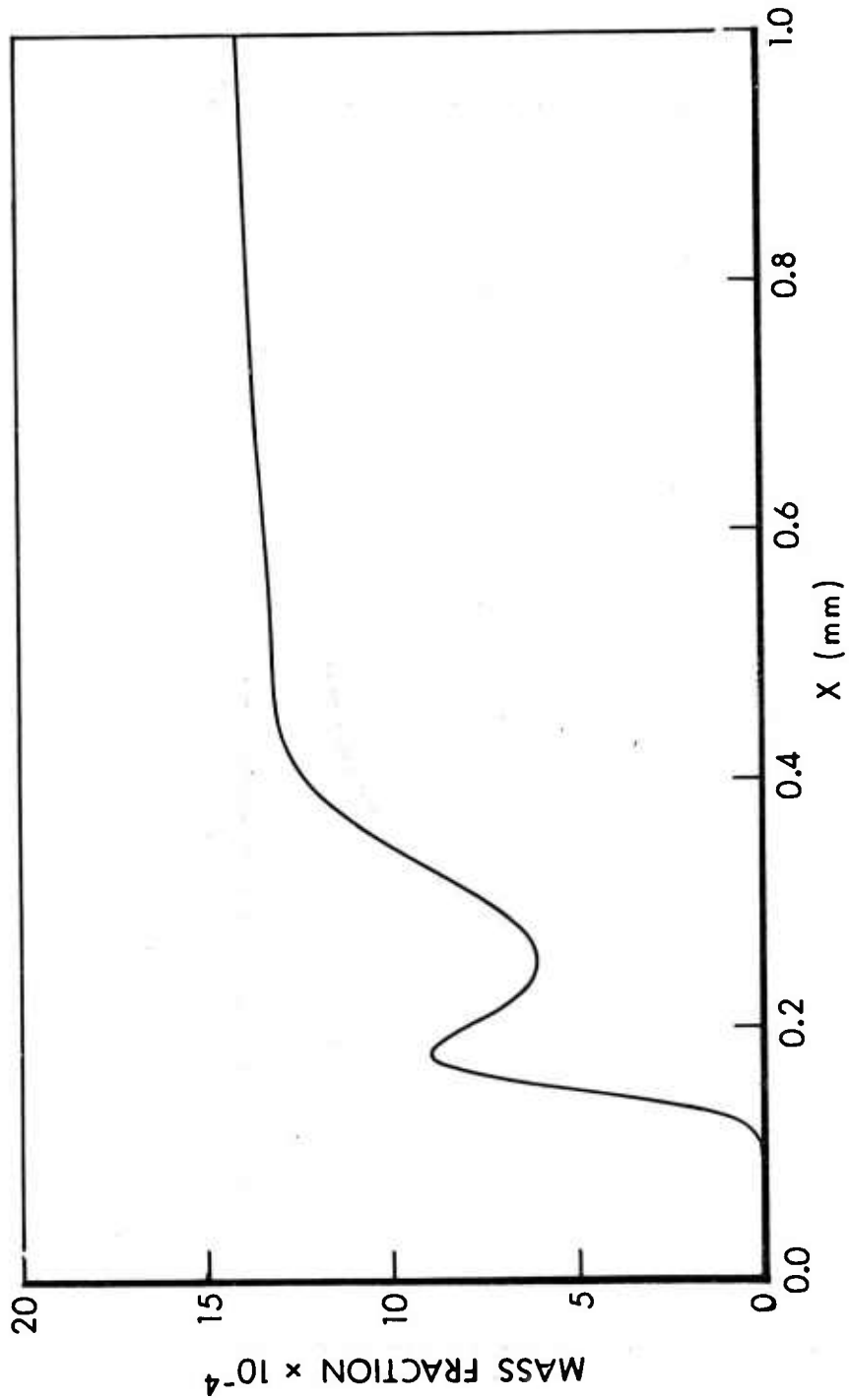

FIGURE 1. OH BENCHMARK PROFILE, FLAME B

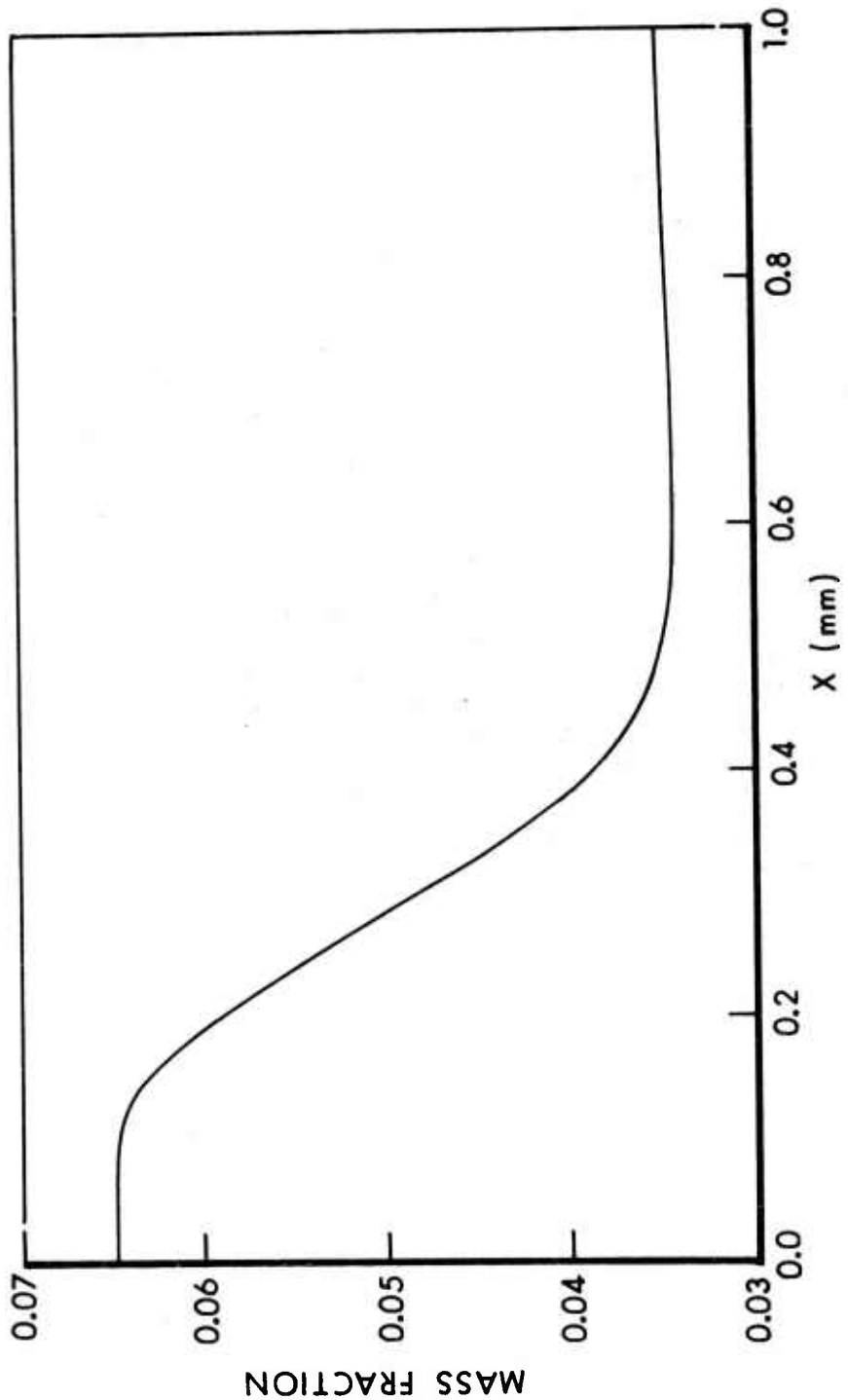

FIGURE 2. H_2 BENCHMARK PROFILE, FLAME B

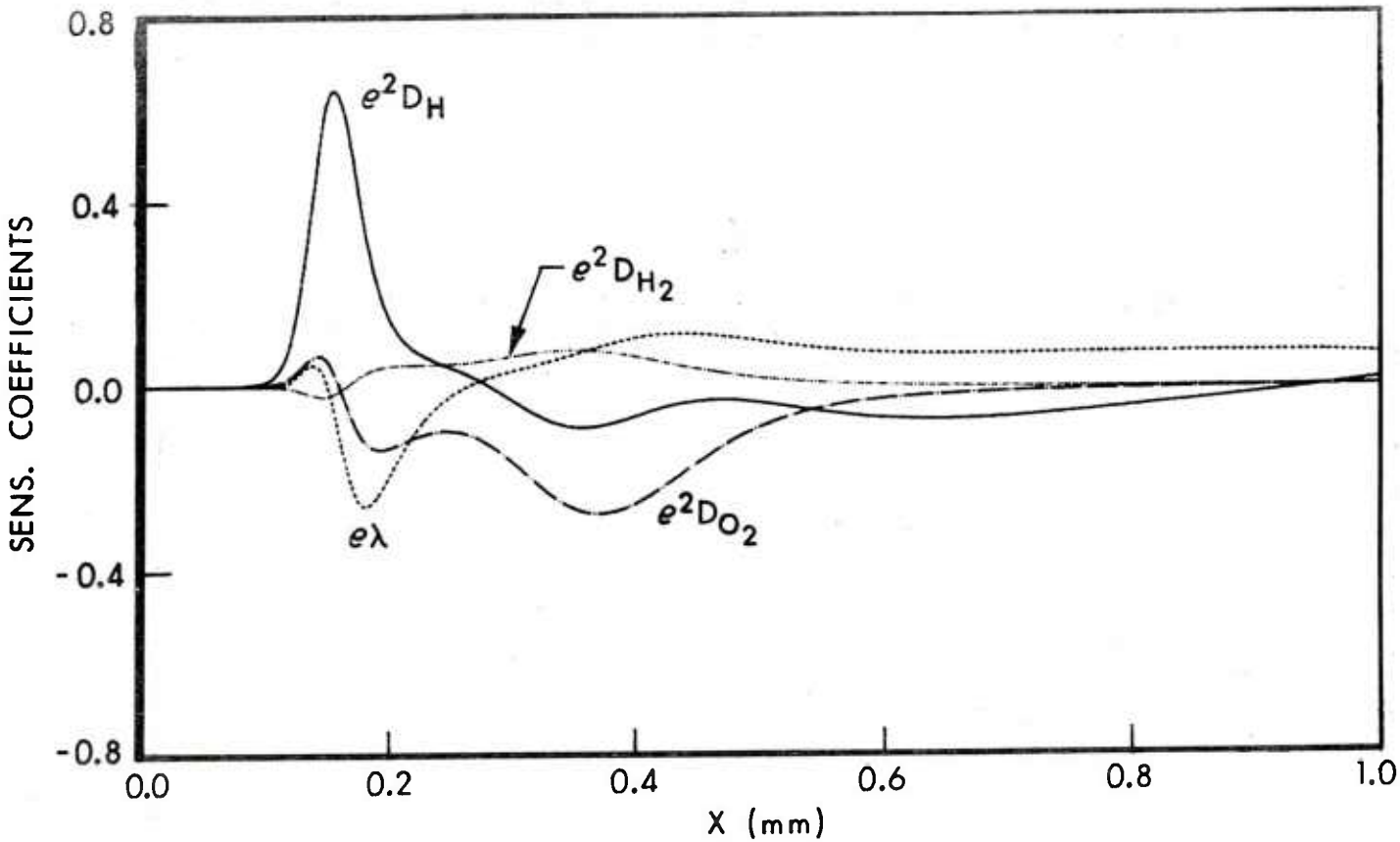

FIGURE 3. NORMALIZED LINEAR SENSITIVITY COEFFICIENTS OF THE OH MASS FRACTION WITH RESPECT TO IMPORTANT TRANSPORT PARAMETERS, FLAME B

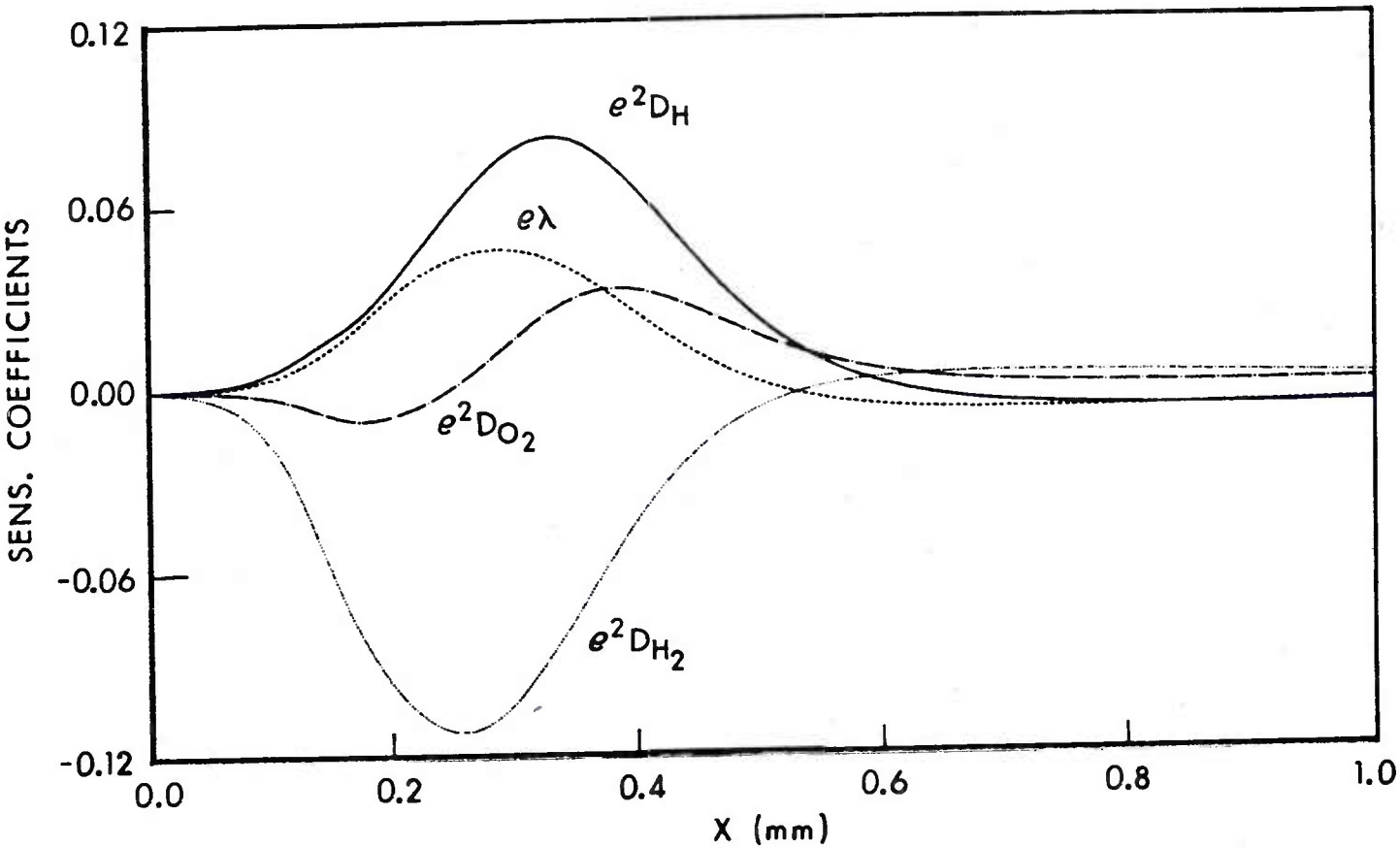

FIGURE 4. NORMALIZED LINEAR SENSITIVITY COEFFICIENTS OF THE H_2 MASS FRACTION WITH RESPECT TO IMPORTANT TRANSPORT PARAMETERS, FLAME B

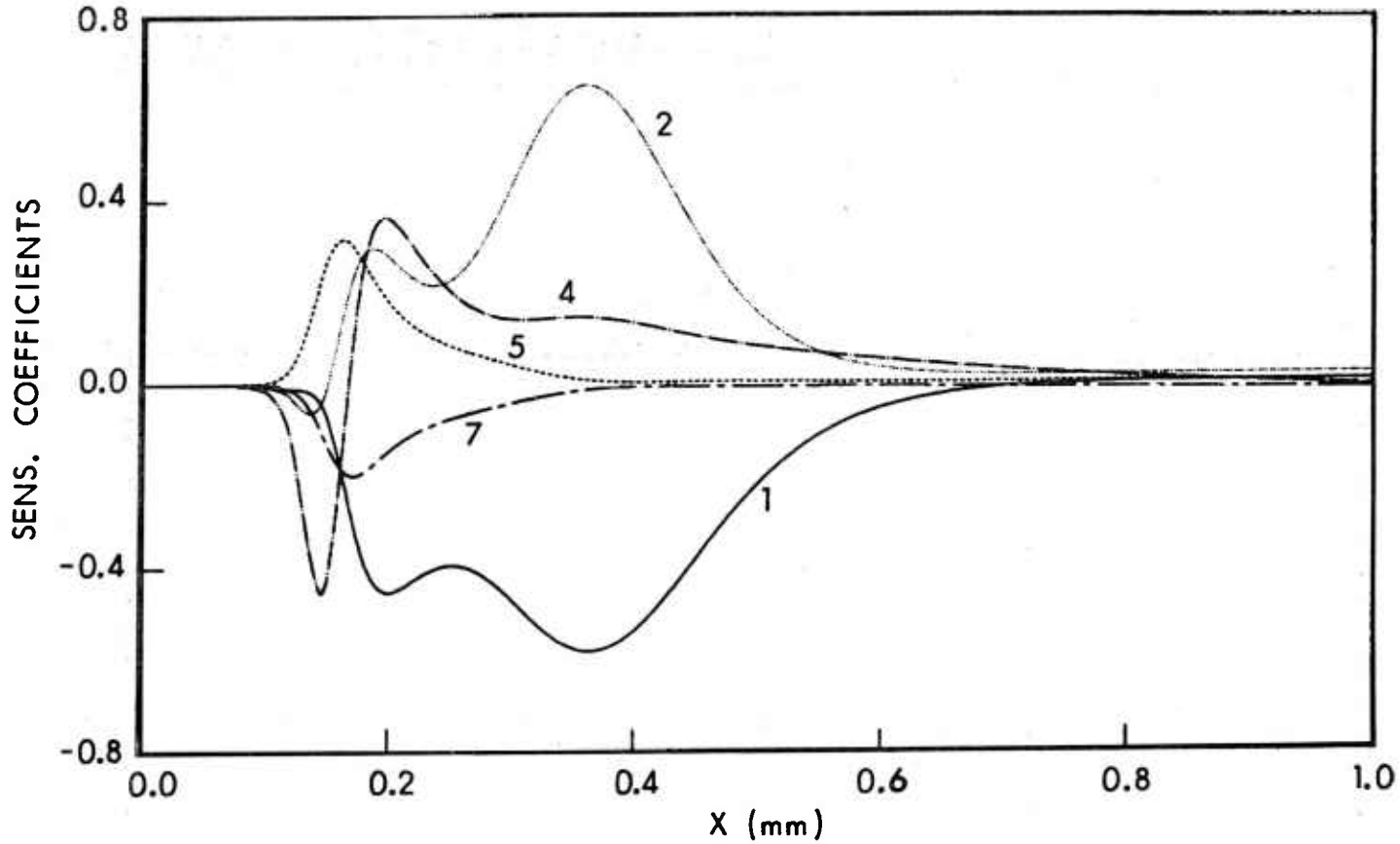

FIGURE 5. NORMALIZED LINEAR SENSITIVITY COEFFICIENTS OF THE OH MASS FRACTION WITH RESPECT TO IMPORTANT REACTION RATE COEFFICIENTS, FLAME B

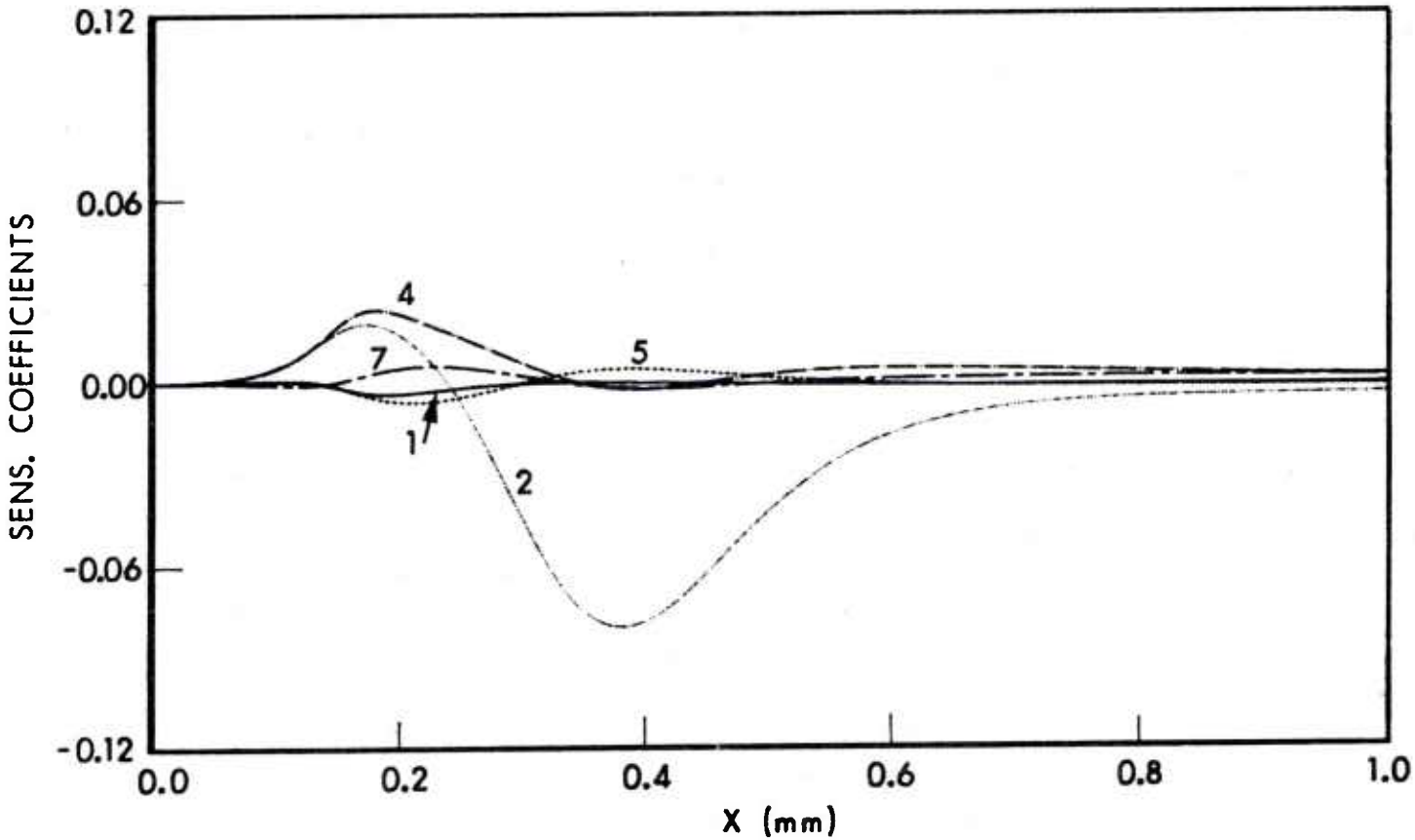

FIGURE 6. NORMALIZED LINEAR SENSITIVITY COEFFICIENTS OF THE H_2 MASS FRACTION WITH RESPECT TO IMPORTANT REACTION RATE COEFFICIENTS, FLAME B

The sensitivity of the flame speed to the input parameters (Tables 3 and 4) is a rough guide to the sensitivity of the profiles. The plotted results show that a species profile is generally sensitive to a number of input parameters. A similar correlation was obtained for the temperature profiles (not shown).

VI. SECOND ORDER SENSITIVITY COEFFICIENTS

In this section we develop a procedure for obtaining second order sensitivity coefficients. The computations are rather complicated and so it would neither be practical nor desirable to carry them out for every problem. The purpose of these second order computations is to establish guidelines for the use of the two linear approximations, Equations (18) and (23). We do this by examining the accuracy and the region of validity for each of the linear approximations.

Since the largest uncertainties are usually associated with the kinetic parameters, we limit this discussion to these parameters. Considering the first and second order terms of a Taylor expansion for the flame speed, we obtain the expression

$$S_N \tilde{=} S_B + \sum_{j=1}^{NR} S^j(\alpha_j - 1) + 0.5 \sum_{j=1}^{NR} S^{jj}(\alpha_j - 1)^2 + \sum_{j=1}^{NR} \sum_{k=j+1}^{NR} S^{jk}(\alpha_j - 1)(\alpha_k - 1), \qquad (30)$$

where

$$S^{jk} = S^{kj} = \partial^2 S / \partial\alpha_j \, \partial\alpha_k \text{ evaluated at } \alpha_j = \alpha_k = 1.$$

Given NR rates, there are NR(NR+1)/2 second order terms.

Equations for the partial derivatives, S^{jk}, are found by taking the partial derivative of Eq. (10) and (11) with respect to α_j and α_k ($1 \le j, k \le NR$) and by letting the α's approach one. The resulting equations are

$$\frac{\partial Y_i^{jk}}{\partial t} + m_o^{jk} \frac{\partial Y_i}{\partial \psi} + m_o^{j} \frac{\partial Y_i^{k}}{\partial \psi} + m_o^{k} \frac{\partial Y_i^{j}}{\partial \psi} + m_o \frac{\partial Y_i^{jk}}{\partial \psi} = \rho^2 D_{im} \frac{\partial^2 Y_i^{jk}}{\partial \psi^2} + \sum_{r=1}^{NR} \left[\delta_{r,j} \left(\frac{R_{ir} M_i}{\rho} \right)^{k} + \delta_{r,k} \left(\frac{R_{ir} M_i}{\rho} \right)^{j} + \left(\frac{R_{ir} M_i}{\rho} \right)^{jk} \right] \qquad (31)$$

and

$$\frac{\partial T^{jk}}{\partial t} + m_o^{jk} \frac{\partial T}{\partial \psi} + m_o^{j} \frac{\partial T^{k}}{\partial \psi} + m_o^{k} \frac{\partial T^{j}}{\partial \psi} + m_o \frac{\partial T^{jk}}{\partial \psi} = \frac{\rho\lambda}{c_p} \frac{\partial T^{jk}}{\partial \psi^2} -$$

$$\frac{1}{c_p} \sum_{i=1}^{N} \sum_{r=1}^{NR} [\delta_{r,j} \{ (\frac{R_{ir} M_i}{\rho})^k h_i + \frac{R_{ir} M_i h_i^k}{\rho} \} + \delta_{r,k} \{ (\frac{R_{ir} M_i}{\rho})^j h_i +$$

$$\frac{R_{ir} M_i h_i^j}{\rho} \} + (\frac{R_{ir} M_i}{\rho})^{jk} h_i + (\frac{R_{ir} M_i}{\rho})^j h_i^k + (\frac{R_{ir} M_i}{\rho})^k h_i^j +$$

$$(\frac{R_{ir} M_i}{\rho})^k h_i^{jk}], \qquad (32)$$

where the superscripts j and k indicate partial derivatives with respect to α_j and α_k, respectively. Explicitly taking the partial derivative we have

$$(\frac{R_{ir} M_i}{\rho})^{jk} = \sum_{m=1}^{N+1} \{ \sum_{n=1}^{N+1} [\partial^2 (\frac{R_{ir} M_i}{\rho}) / \partial u_m \partial u_n] u_m^j u_n^k +$$

$$[\partial (\frac{R_{ir} M_i}{\rho}) / \partial u_m] u_m^{jk} \}. \qquad (33)$$

The benchmark values and the first order sensitivity coefficients are known, and the boundary conditions for this system of equations is

$$u_m^{jk} = 0 \quad \text{at } \psi = -\infty \quad (x=-\infty)$$

and (34)

$$\partial u_m^{jk} / \partial \psi = 0 \text{ at } \psi = +\infty \quad (x = +\infty).$$

Thus Eq. (31) and (32) can be solved for the m_o^{jk} and u_m^{jk}.

Expanding Eq. (24) in terms of the $\ln\alpha_j$ up to second order, we obtain

$$\ln S_N \tilde{=} \ln S_B + \sum_{j=1}^{NR} S_E^j \ln \alpha_j + 0.5 \sum_{j=1}^{NR} S_E^{jj} (\ln\alpha_j)^2 + \sum_{j=1}^{NR} \sum_{k=j+1}^{NR} S_E^{jk} \ln\alpha_j \ln\alpha_k. \qquad (35)$$

An equivalent form of Eq. (35) is

$$S_N \tilde{=} S_B \prod_{j=1}^{NR} \alpha_j^{(S_E^j + 0.5 \sum_{k=1}^{NR} S_E^{jk} \ln\alpha_k)}. \qquad (36)$$

As with the linear coefficients, we can find an expression relating the second order sensitivity coefficients of the polynomial expansion, Eq. (30) and the sensitivity exponents of Eq. (35). The partial derivative of Eq. (35) with respect to α_m yields

$$\frac{\partial S_N/\partial \alpha_m}{S_N} = \frac{S_E^m}{\alpha_m} + \frac{S_E^{mm} \ln \alpha_m}{\alpha_m} + \sum_{k \neq m} \frac{S_E^{mk} \ln \alpha_k}{\alpha_m} . \qquad (37)$$

By taking the partial of Eq. (37) with respect to α_m and by letting the α's approach 1, we obtain

$$S_E^{m\,m} = \frac{S^{m\,m}}{S_B} + S_E^m - (S_E^m)^2 . \qquad (38)$$

Similarly, by taking the partial with respect to α_n, $n \neq m$,

$$S_E^{m\,n} = \frac{S^{m\,n}}{S_B} - S_E^m S_E^n . \qquad (39)$$

Inspection of Equations (38) and (39) shows that the second order logarithmic coefficients, S_E^{mn}, are related to the second order normalized derivatives, $S^{mn} = \partial^2 S/\partial\alpha_m \partial\alpha_n$, in a more complicated fashion than the corresponding relationship between first order coefficients given by Eq. (28). Specifically it is possible for S_E^{mn} to be large or small relative to S^{mn}/S_B. In general, the expansion (30) in terms of $(\alpha_j - 1)$ and the expansion (35) in terms of $\ln \alpha_j$ will have different rates of convergence.

In the special case $\alpha_1 = \ldots = \alpha_{NR}$, the linear logarithmic expansion, Eq. (24) is exact and Eq. (25) holds. Thus all higher order terms of the expansion for lnS must sum to zero. For the present case of a second order expansion we have from Eq. (35) that

$$0.5 \sum_{j=1}^{NR} S_E^{jj} + \sum_{j=1}^{NR} \sum_{k=j+1}^{NR} S_E^{jk} = 0. \qquad (40)$$

VII . SECOND ORDER ANALYSIS NUMERICAL RESULTS AND DISCUSSION

1. Flame Speed.

The main difficulty with second order analysis is the large number of terms. For example in the present case of 17 reaction rate coefficients there exist 153 second order terms. Therefore, in our examples, second order coefficients were computed only for the reactions that were found important by the first order analysis. Table 5 lists a subset of the flame speed sensitivity coefficients computed for flame B. Table 6 lists those for flame D. Both the logarithmic sensitivity coefficients, S_E^{jk}, and the normalized polynomial coefficients, S^{jk}/S_B, are given for comparison.

TABLE 5. SELECTED FLAME SPEED FIRST AND SECOND ORDER SENSITIVITY COEFFICIENTS FOR THE RATE COEFFICIENTS OF FLAME B.

j	k	S_E^j	S_E^{jk}	S^{jk}/S_B
1	1	.0744	-.0477	-.1166
	2		.0356	.0572
	4		.0123	.0259
	5		.0232	.0314
	7		-.0227	-.0298
2	2	.2911	-.1211	-.3275
	4		.0203	.0738
	5		-.0361	-.0041
	7		.0390	.0113
4	4	.1838	-.0493	-.1993
	5		.0310	.0512
	7		-.0248	-.0423
5	5	.1099	-.0454	-.1432
	7		.0493	.0388
7	7	-.0952	-.0624	.0419

$$0.5 \sum S_E^{jj} + \sum_{j \neq k} \sum S_E^{jk} = -.0359$$

$$0.5 \sum |S_E^{jj}| + \sum_{j \neq k} \sum |S_E^{jk}| = .4573$$

TABLE 6. SELECTED FLAME SPEED FIRST AND SECOND ORDER SENSITIVITY COEFFICIENTS FOR THE RATE COEFFICIENTS OF FLAME D.

j	k	S_E^j	S_E^{jk}	S^{jk}/S_B
1	1	.0576	-.0489	-.1032
	2		.0692	.1409
	4		-.0126	-.0432
	5		.0489	.0920
	7		-.0648	-.1084
2	2	1.2427	-.0815	-.4999
	4		.6547	-.0054
	5		-.5327	.3984
	7		.6015	-.3373
4	4	-.5312	-.7089	.1044
	5		.4922	.0943
	7		-.5160	-.1146
5	5	.7492	-.2916	-.4795
	7		.3797	-.1863
7	7	-.7555	-.4701	.8562

$$0.5 \sum S_E^{jj} + \sum_{j \neq k} \sum S_E^{jk} = -.0404$$

$$0.5 \sum |S_E^{jj}| + \sum_{j \neq k} \sum |S_E^{jk}| = 4.5328$$

The values of the flame speed sensitivity coefficients, S_E^{ii}, are negative for all four flames. This can be interpreted by considering a simplified case. Consider the single rate coefficient, j, with $S_E^j > 0$ and $\alpha_j > 1$. Then the flame speed will increase. Physically we know that, for those flames that involve a chain of reactions, as is the case here with hydrogen/oxygen, the faster a reaction becomes the more sensitive the flame speed becomes to other, slower reactions in the chain. At some point further increases in the jth rate coefficient have little effect upon the flame speed. Numerically then we expect that the first order logarithmic approximation overestimates the flame speed and that the second order correction should be negative. By the symmetry of Eq. (23), the argument also holds if $S_E^j < 0$ and the rate coefficient is decreased, i.e. $\alpha_j < 1$.

Continuing with our example, we find that from Eqs. (18) and (28) the linear Taylor expansion in terms of $(\alpha_j - 1)$ can be written as

$$S_N(\text{Tay}) = S_B[1+S_E^j (\alpha_j - 1)]. \tag{41}$$

The logarithmic formula, Eq. (23), is also expanded in terms of $(\alpha_j - 1)$ and the results are

$$S_N(\text{Log}) = S_B\alpha_j^{S_E^j} = S_B[1+S_E^j (\alpha_j-1) + S_E^j(S_E^j-1) (\alpha_j-1)^2 /2 + \ldots]. \tag{42}$$

From Eqs. (41) and (42) we see that the two approximations are identical whenever $S_E^j = 0$ or $S_E^j = 1$. This leads us to consider three regions of interest: 1) $0 < S_E^j < 1$, 2) $S_E^j > 1$, and 3) $S_E^j < 0$.

The difference between the approximations given by Eqs. (41) and (42) is

$$S_N(\text{Log}) - S_N(\text{Tay}) = S_E^j(S_E^j - 1) (\alpha_j - 1)^2/2, \tag{43}$$

where we have assumed that third order and higher terms in Eq. (42) are negligible. For the case $0 < S_E^j < 1$ we see from Eq. (43) that

$$S_n(\text{Log}) < S_N(\text{Tay}). \tag{44}$$

We have argued above that the first order logarithmic approximation, $S_N(\text{Log})$, will overestimate the flame speed; then, from Eq. (44), we expect that the approximation given by Eq. (41) for $S_N(\text{Tay})$ will be even worse.

We can check this heuristic argument. Were the linear approximation in terms of $\ln\alpha_j$ in fact better than the linear approximation in terms of $(\alpha_j - 1)$, then the second order term in the logarithmic expansion, $|S_E^{jj}|$ ought to be smaller than the normalized second order term $|S^{jj}/S_B|$. Inspection of the

values listed in Tables 5 and 6 support this conclusion; i.e. that $|S_E^{jj}| < |S^{jj}/S_B|$ whenever $0 < S_E^j < 1$.

For the cases $S_E^j > 1$ or $S_E^j < 0$ we see from Eq. (43) that $S_N(\text{Log}) > S_N(\text{Tay})$. In these cases we expect the Taylor expansion, Eq. (41), to be more accurate than the logarithmic expansion, Eq. (42).

The above inferences for a single rate coefficient, can be summarized and generalized to more than one parameter. For a flame with $0 < S_E^j < 1$ for most S_E^j, (e.g. flame B), the overall sensitivity, $\Sigma|S_E^j|$, will be relatively small and the logarithmic expansion will be more accurate. On the other hand, if $\Sigma|S_E^j|$ is large (e.g. Flame D) then both expansions will be accurate only for small departures of the α_j from unity and the expansion in terms of $(\alpha_j - 1)$, Eq. (18), will have a wider range of validity.

In addition one can have $\Sigma S_E^j \sim 0.5$ and $\Sigma|S_E^j|$ large only if there are many S_E^j of opposite signs. We conclude from this that the larger the overall sensitivity, the more complex the factors affecting the output functions are expected to be.

In passing we note that the magnitude of the second order terms indicates the degree of coupling between corresponding reactions. For flame B, the largest S_E^{jk}, $j \neq k$, is S_E^{57}. Reactions 5 and 7 directly compete for the consumption of HO_2, which has a small concentration. For flame D, the reactions 2,4,5 and 7 are all closely coupled because of the small concentrations of H in this flame. A change in any one of the above rate coefficients strongly affects the other three.

2. Profiles.

We are also interested in the behavior of the profiles. As examples, results for the OH and H_2 profiles, flame B, will again be used. Figures 7 and 8 show the second order sensitivity coefficients: u_i^{11}, u_i^{12}, u_i^{22}, and u_i^{44} for OH and H_2, respectively; the coefficients have been normalized by dividing by the maximum of each benchmark profile, $u_{iB}(\text{max})$. Figures 9 and 10 show the corresponding logarithmic coefficients. These are related to the coefficients of the expansion in terms of $(\alpha_j - 1)$; see Eqs. (38) and (39). In order to compare the two sets of second order coefficients, the u_E^{jk} are first multiplied by u_{iB} before normalizing by dividing by $u_{iB}(\text{max})$. The other sensitivity coefficients for flame B are not shown because they are small relative to those shown in Figures 7-10.

Since the normalized second order logarithmic sensitivity coefficients are smaller than the first order coefficients and since the second order coefficients from the polynomial expansion have about the same magnitude as the first order coefficients, we conclude that, in this example, the logarithmic formula, Eq. (24), is more accurate than the linear polynomial formula, Eq. (18).

There is no longer any strong correlation between large flame speed sensitivity coefficients and large profile sensitivity coefficients.

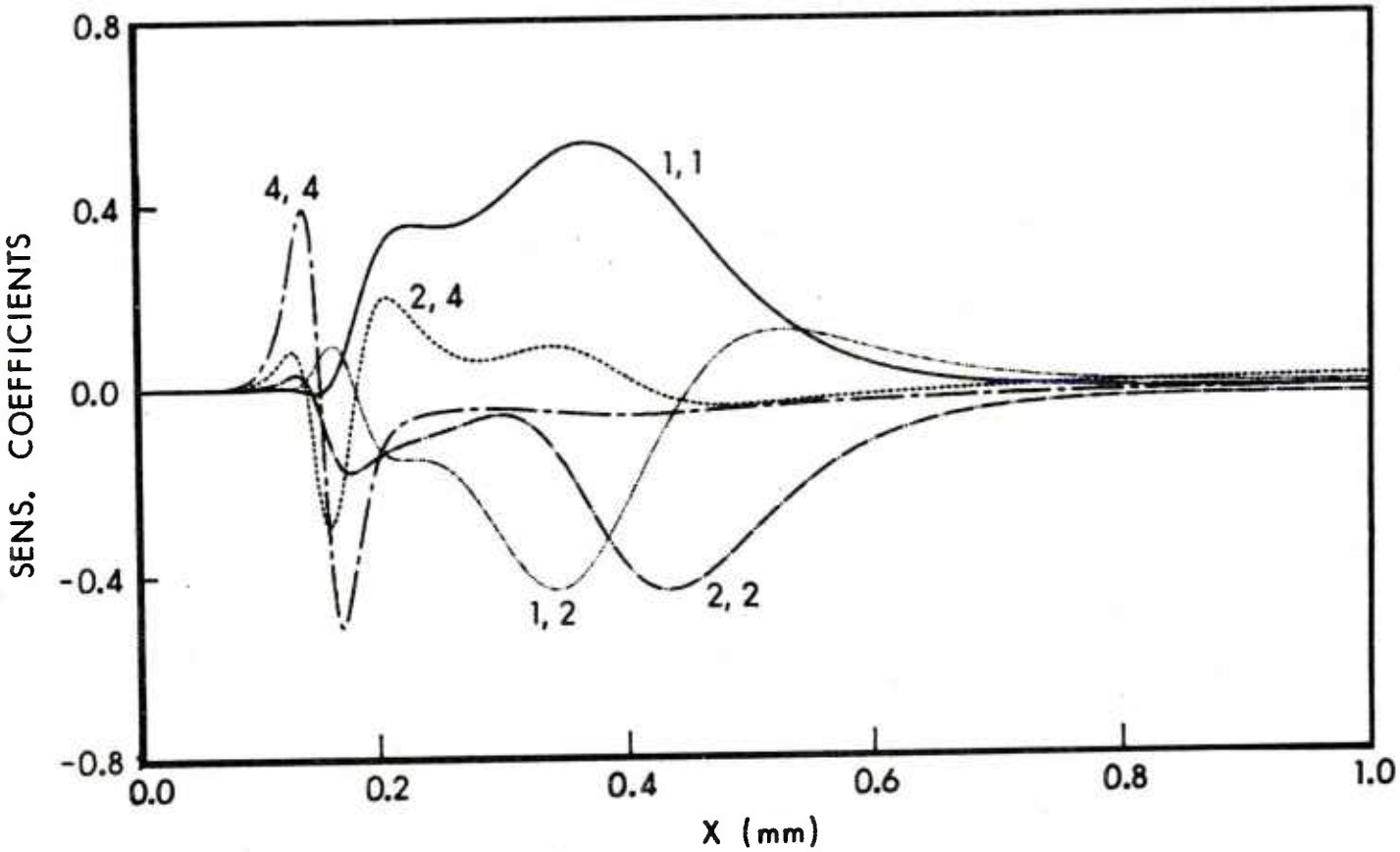

FIGURE 7. NORMALIZED SECOND ORDER SENSITIVITY COEFFICIENTS OF THE OH MASS FRACTION WITH RESPECT TO IMPORTANT REACTION RATE COEFFICIENTS, FLAME B

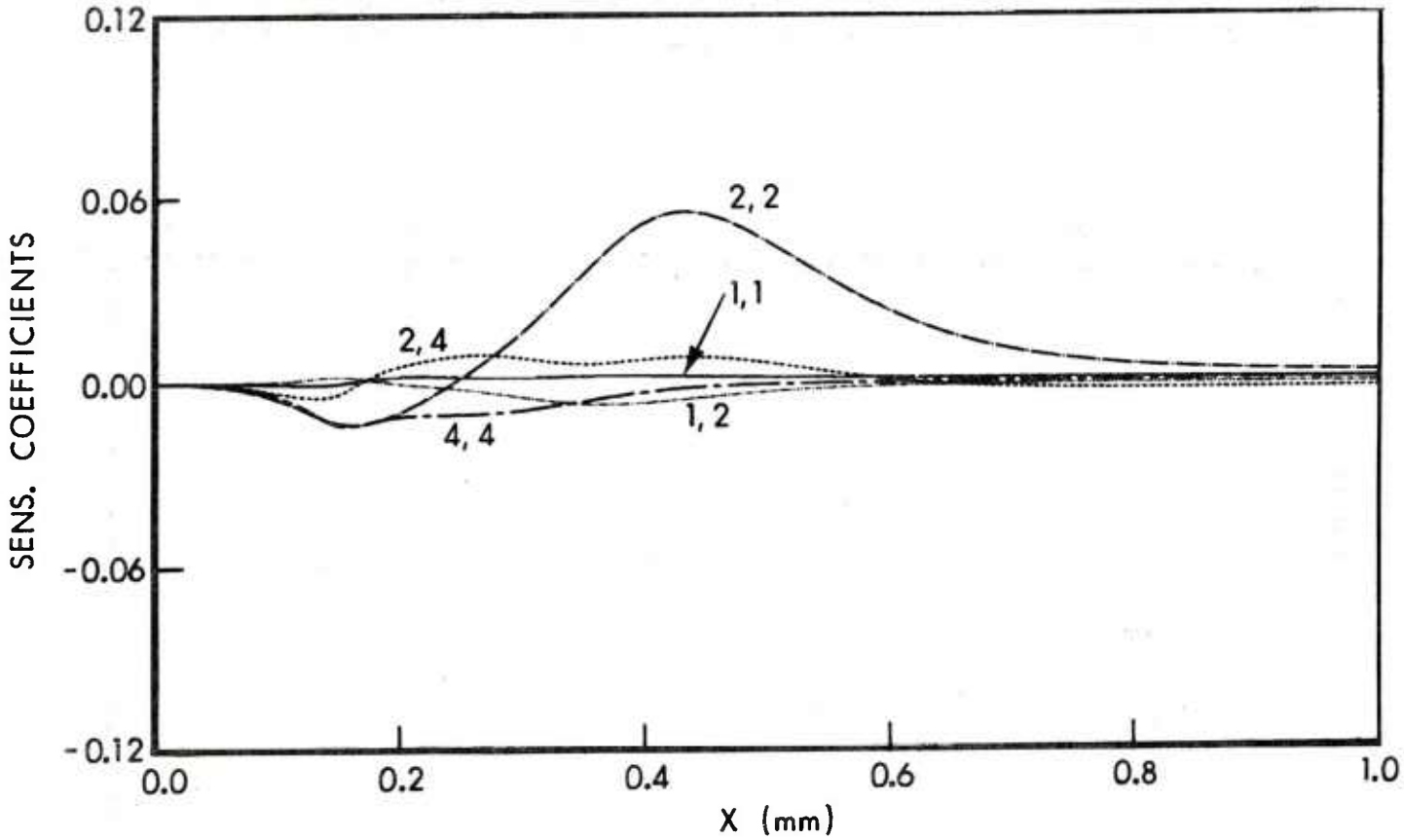

FIGURE 8. NORMALIZED SECOND ORDER SENSITIVITY COEFFICIENTS OF THE H_2 MASS FRACTION WITH RESPECT TO IMPORTANT REACTION RATE COEFFICIENTS, FLAME B

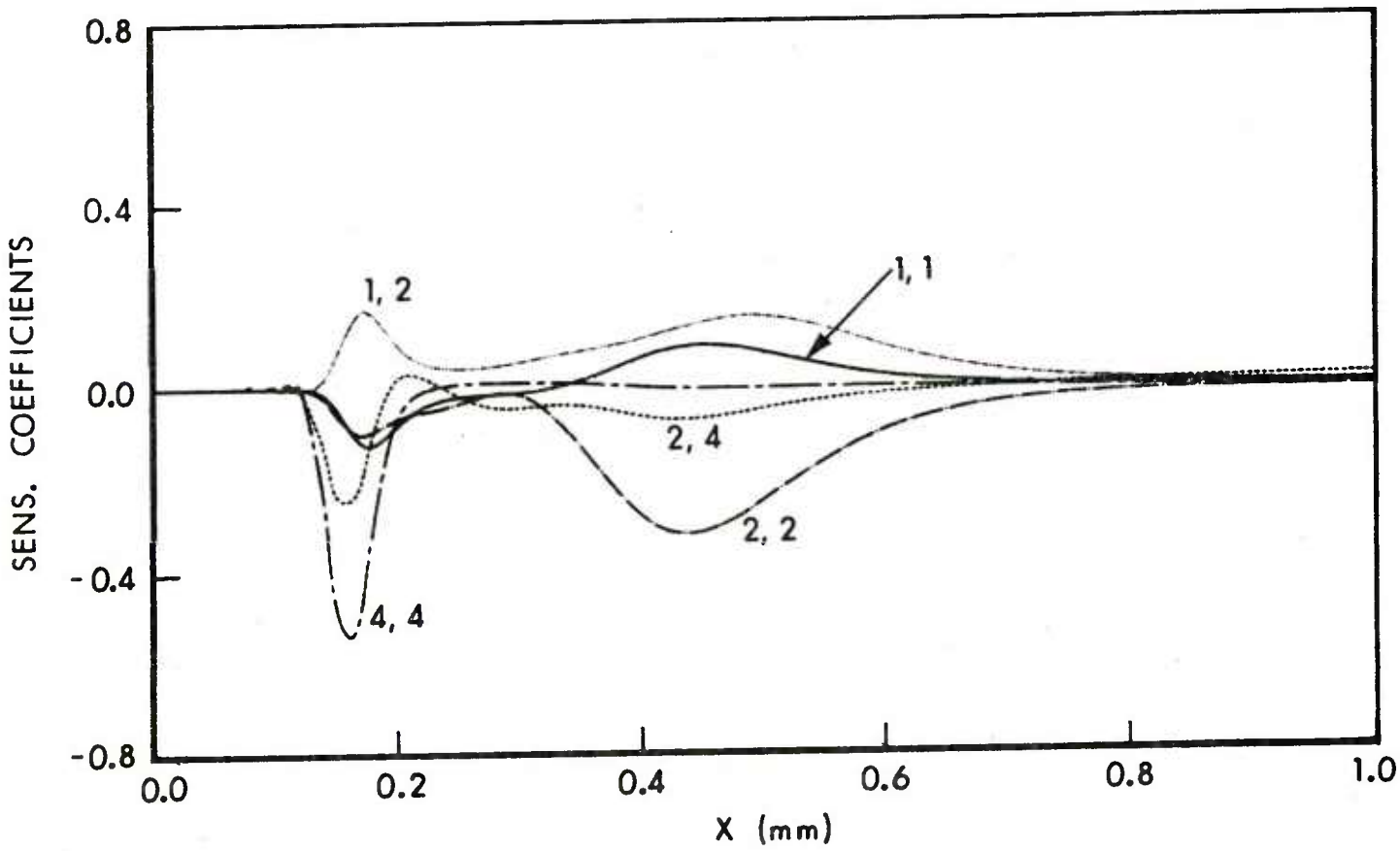

FIGURE 9. NORMALIZED SECOND ORDER LOGARITHMIC COEFFICIENTS OF THE OH MASS FRACTION WITH RESPECT TO IMPORTANT REACTION RATE COEFFICIENTS, FLAME B

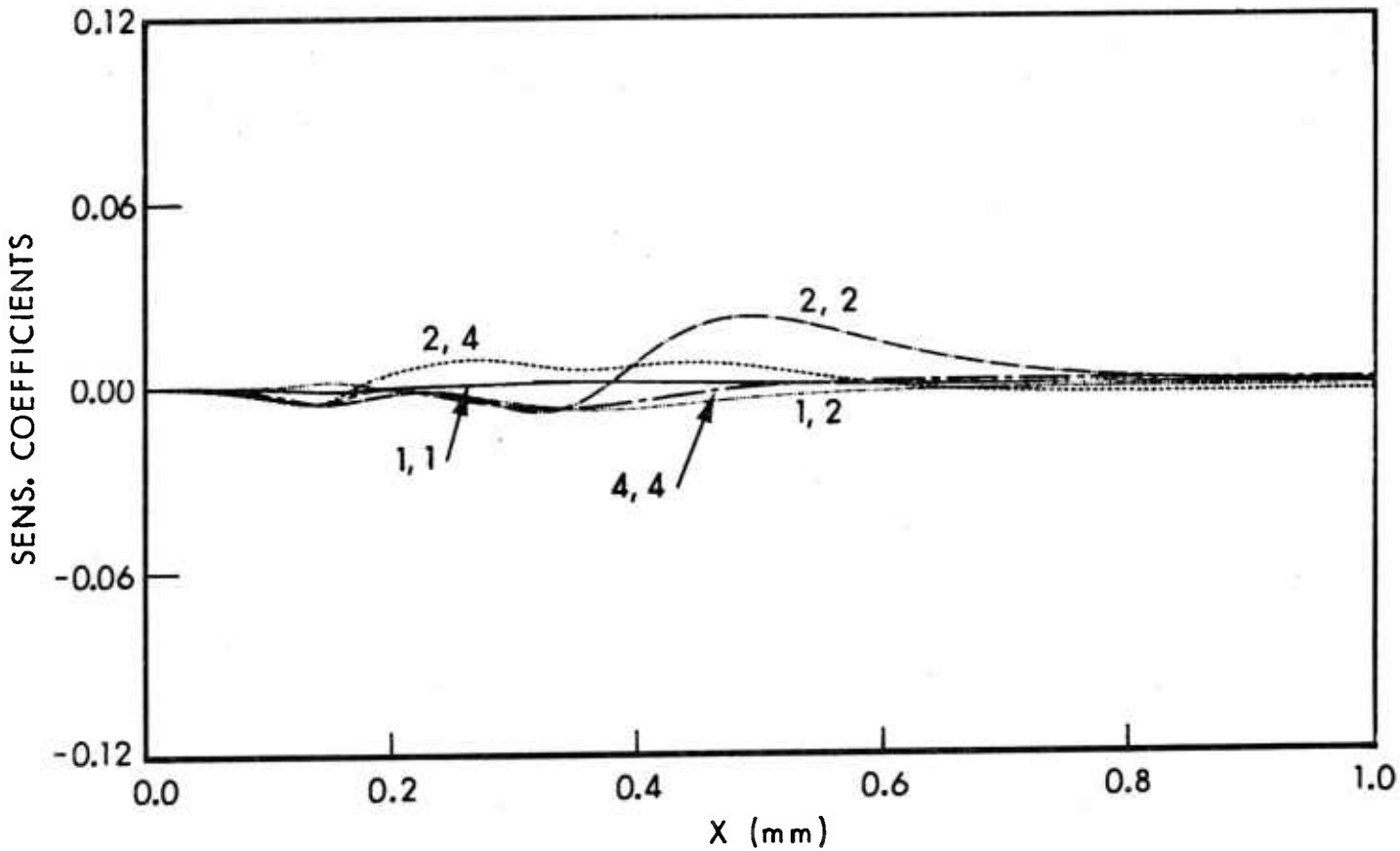

FIGURE 10. NORMALIZED SECOND ORDER LOGARITHMIC COEFFICIENTS OF THE H_2 MASS FRACTION WITH RESPECT TO IMPORTANT REACTION RATE COEFFICIENTS, FLAME B

For flames A and C (not shown) the results are similar to those for flame B.

The second order sensitivity coefficients of the OH profile for flame D (not shown) exhibit the following behavior. The second order polynomial coefficients are larger than the first order coefficients and the second order logarithmic coefficients are even larger. There are many coupling terms with large values, a situation similar to the flame speed coefficients of Table 6. For the H_2 profile (not shown), the second order polynomial coefficients are somewhat smaller than the first order coefficients and the logarithmic coefficients smaller still.

In summary we find the results of these sensitivity analyses follow those for the flame speeds. Specifically, for flames A, B and C we find that the logarithmic formula is the more accurate. We also find this to be the case for the major species and the temperature of flame D. However, for the radical profiles of flame D, where the first order coefficients are large (i.e. of order two), then both expansions will be accurate only for small departures of the α_j from unity. The expansion in terms of the $(\alpha_j - 1)$ will have the wider range of validity.

VIII. COMPARISONS OF EXTRAPOLATIONS

So far we have developed four possible extrapolations based on sensitivity coefficients. The expansions in terms of $(\alpha_j - 1)$ we shall call Linear Taylor and Second Order Taylor. The expansions in terms of $\ln\alpha_j$ we shall call Linear Logarithmic and Second Order Logarithmic. In this section these extrapolations are compared with exact numerical solutions for selected values of α_j. The purpose is to quantify the heuristic arguments made in the last section.

Changes of a factor of two in the input parameters will be considered. This degree of uncertainty is typical for many rate coefficients, and is large enough that a linear expansion can be inaccurate.

Tables 7 and 8 give a few typical results for burning velocity for flame B. We consider rate coefficient 2, which has the largest positive linear sensitivity coefficient, rate coefficient 7, which has the largest negative linear sensitivity coefficient, combinations of rate coefficients 2 and 7, and combinations of several other rate coefficients. The percent error is computed by dividing the difference of the numerical value and the extrapolated value by the benchmark value found in Table 2, and multiplying by one hundred.

TABLE 7. COMPARISONS OF COMPUTED AND EXTRAPOLATED FLAME SPEEDS. FLAME B. LINEAR EXPANSIONS.

j	α_j	Numerical	Taylor	Logarithmic	%	Errors
2	2.0	299.2	325.3	308.3	10.4	3.6
2	0.5	200.1	215.3	205.9	6.0	2.3
7	2.0	232.3	228.0	235.8	1.7	1.4
7	0.5	265.4	263.9	269.1	0.6	1.5
2 7	2.0 0.5	311.5	337.3	329.3	10.2	7.1
2 7	0.5 2.0	179.5	191.3	192.8	4.7	5.3
1,2,4,5	2.0	388.7	418.0	397.9	11.6	3.6
1,2,4,5	0.5	156.2	168.9	159.5	5.0	1.3
1,2,4,5 7	2.0 0.5	403.0	430.0	425.0	10.7	8.7
1,2,4,5 7	0.5 2.0	141.6	144.9	149.3	1.3	3.1

TABLE 8. COMPARISONS OF COMPUTED AND EXTRAPOLATED FLAME SPEEDS. FLAME B. SECOND ORDER EXPANSIONS

j	α_j	Numerical	Taylor	Logarithmic	%	Errors
2	2.0	299.2	284.0	299.4	6.0	0.1
2	0.5	200.1	205.0	200.0	1.9	0.1
7	2.0	232.3	233.2	232.3	0.4	0.0
7	0.5	265.4	265.2	265.1	0.1	0.1
2 7	2.0 0.5	311.5	295.9	309.2	6.2	0.9
2 7	0.5 2.0	179.5	184.8	181.0	2.1	0.6
1,2,4,5	2.0	388.7	378.3	389.3	4.2	0.2
1,2,4,5	0.5	156.2	159.0	156.1	1.1	0.1
1,2,4,5 7	2.0 0.5	403.0	394.3	401.7	3.5	0.5
1,2,4,5 7	0.5 2.0	141.6	143.0	141.2	0.6	0.2

All four extrapolations are accurate. In general, the linear logarithmic extrapolation is more accurate than the linear Taylor extrapolation. The only exceptions are some cases involving rate coefficient 7. This is expected from the analysis in Section VII. In all examples, the second order logarithmic extrapolation is more accurate than the second Taylor formula. Additional cases were computed for flame B and for flames A and C and the results are similar to these given here.

Flame D, as usual, is an exception. Tables 9 and 10 contain some results for the four rate coefficients with the largest sensitivity coefficients. The errors in the extrapolations are larger than before, although still mostly reasonable. The linear logarithmic extrapolation is slightly more accurate for changes in rate coefficient 5 ($S_E^5 = .7492$).

TABLE 9. COMPARISONS OF COMPUTED AND EXTRAPOLATED FLAME SPEEDS. FLAME D. LINEAR EXPANSIONS.

j	α_j	Numerical	Taylor	Logarithmic	%	Errors
2	2.0	23.6	26.5	28.0	24.5	36.9
2	0.5	4.1	4.5	5.0	3.5	7.9
4	2.0	6.6	5.6	8.2	9.1	13.2
4	0.5	14.9	15.0	17.1	0.8	18.8
5	2.0	18.6	20.7	19.9	18.0	11.2
5	0.5	6.6	7.4	7.0	6.4	3.4
7	2.0	6.3	2.9	7.0	28.9	5.9
7	0.5	18.0	16.3	20.0	14.1	17.0
2,5 4,7	2.0 0.5	35.2	43.0	114.8	65.8	672.7
2,5 4,7	0.5 2.0	0.0	-15.2	1.2	128.3	10.3

TABLE 10. COMPARISONS OF COMPUTED AND EXTRAPOLATED FLAME SPEEDS. FLAME D. SECOND ORDER EXPANSIONS.

j	α_j	Numerical	Taylor	Logarithmic	%	Errors
2	2.0	23.6	23.6	23.1	0.5	4.6
2	0.5	4.1	3.7	4.1	2.8	0.5
4	2.0	6.6	6.2	6.9	3.9	2.4
4	0.5	14.9	15.1	14.4	2.1	3.9
5	2.0	18.6	17.9	18.5	6.0	0.2
5	0.5	6.6	6.7	6.6	0.4	0.7
7	2.0	6.3	8.0	6.3	13.9	0.5
7	0.5	18.0	17.6	17.8	3.4	1.0
2,5 4,7	2.0 0.5	35.2	45.6	14.5	87.5	175.5
2,5 4,7	0.5 2.0	0.0	-8.6	0.2	72.2	1.3

For rate coefficient 2, ($S_E^2 > 1$) and rate coefficients 4 and 7 ($S_E^4 < 0$, $S_E^7 < 0$), the linear Taylor extrapolation is usually more accurate as expected from the analysis in Section VIII. The exception is $\alpha_7 = 2$. This change is large enough so that the asymptotic behavior of the formulas becomes important. If $S_E^j < 0$, as $\alpha_j \to \infty$ the linear Taylor extrapolation approaches $-\infty$ while the logarithmic extrapolation approaches 0. So for large decreases in the flame speed (or mass fraction or temperature) the logarithmic extrapolation will be more accurate.

When the above rate coefficients 2,5,4 and 7 are changed, both extrapolations have problems. If the changes are made so as to increase the flame speed, the linear Taylor formula is still reasonably accurate. However, the second order approximation is less accurate than the first. The linear logarithmic extrapolation is much too large. Since it is an exponential function, it is possible to badly overestimate for a set of large S_E^j's. However, the second order expansion does represent improved accuracy.

If the changes in the rates are made so as to decrease the flame speed, the asymptotic properties of the formulas become important. The numerical solution indicates extinction of the flame. The linear Taylor expansion terms predict a negative flame speed, while the logarithmic formula can produce only non-negative speeds. So while the Taylor formula may be more accurate for small decreases in the burning velocity, the logarithmic formula is more accurate for large decreases.

Again, we use flame B as an example in considering the profiles. The case $\alpha_1 = \alpha_2 = \alpha_4 = \alpha_5 = 2.0$, $\alpha_7 = 0.5$, will be considered.

Figure 11 shows the linear extrapolations. The Taylor expansion predicts negative values near the cold boundary, which are cut off in the graph. The logarithmic expansion follows the numerical solution better here.

At the first peak the OH mass fraction increases substantially. Here the Taylor series is more accurate, although both series overestimate the correct value. This can happen when a concentration increases by a large amount. In the flame front and post flame region, the logarithmic formula is more accurate.

Figure 12 we see that the second order logarithmic extrapolation is much more accurate than the second order Taylor expansion. In fact, the Taylor expansion overcorrects badly at several locations. For instance near x = 0.1, the negative values of the linear extrapolations have become a spurious OH peak.

Figure 13 and 14 show the H_2 results over all the logarithmic expansions are more accurate.

A number of additional cases (not shown) were run for flames A,B, and C. For the major species and temperature, the logarithmic extrapolation was more accurate for all the cases considered. For the radical species, the linear logarithmic formula was usually more accurate than the linear terms of the Taylor expansion, but there were exceptions. The second order logarithmic approximation always was more accurate than the second order Taylor approximation.

For flame D, the first order logarithmic formula for the radical species was very inaccurate. Since radical concentrations were small, any change in the rate coefficients tended to cause a large change in the radical profiles (i.e. $u_{iE}^J > 1$). Even the second order logarithmic formula was less accurate than the second order Taylor approximation .

For the major species and temperature profiles, the first order logarithmic formula was substantially more accurate than the first order Taylor formula.

XI. SUMMARY AND CONCLUSIONS

By employing expansions in terms of ($\alpha_j - 1$) and $\ln\alpha_j$, we have developed methods and the corresponding computer programs to obtain first and second order sensitivity coefficients. The codes are straightforward to execute, but, for large sets of variable parameters, can be computationally expensive.

We have applied these sensitivity analyses to a test case of a set of $H_2/O_2/N_2$ flames that span a wide range of flame speeds and fuel-oxidizer ratios. We found that the linear sensitivity coefficients for the flame speeds by themselves give a good overall description of the important input parameters. Conversely, they would also permit a given complex kinetic mechanism to be understood. (This type of sensitivity analysis bridges the gap between a fixed, determined set of numbers obtained from a numerical code and the functional relationships that show trends, obtained from analytic

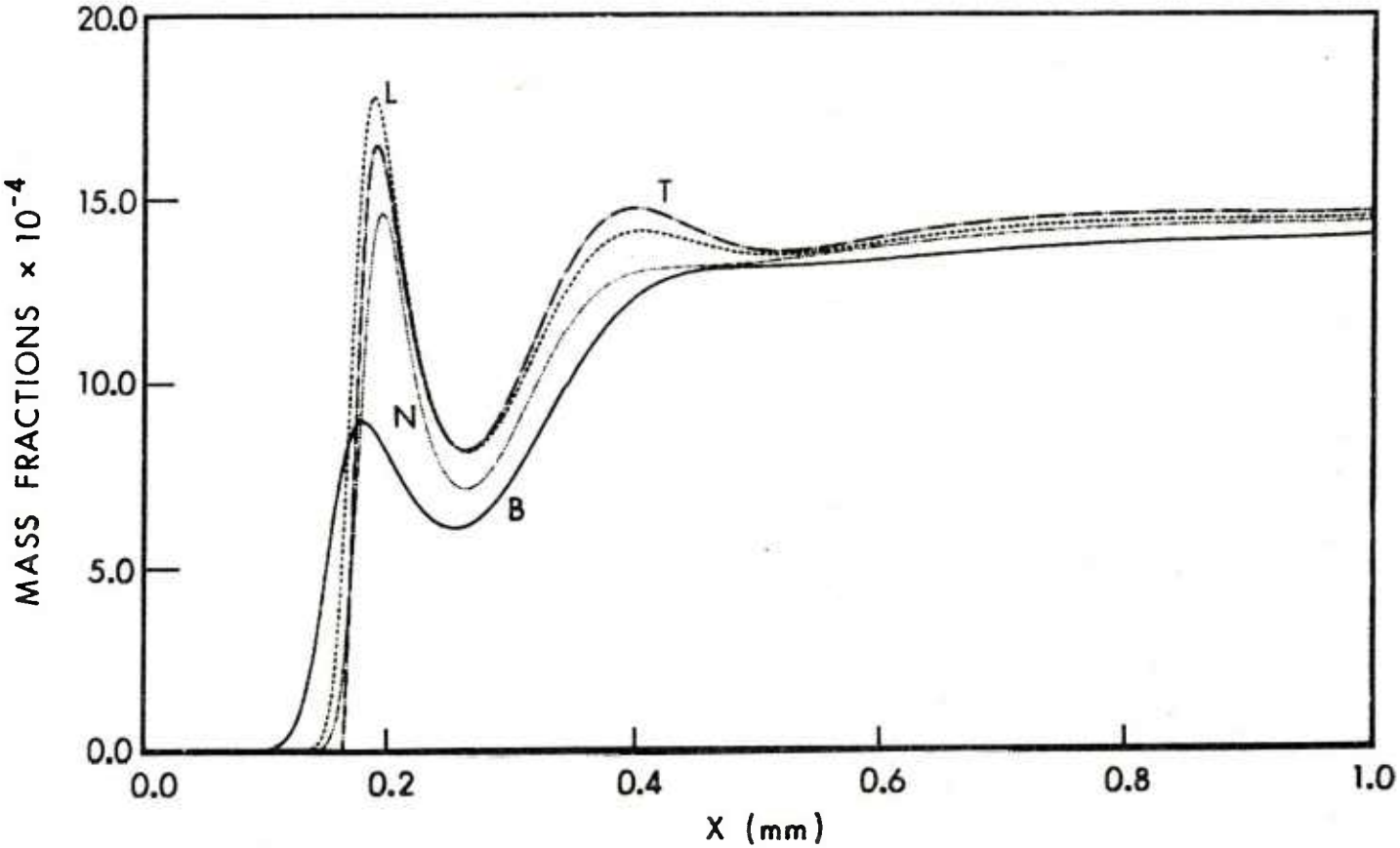

FIGURE 11. OH MASS FRACTION PROFILE, FLAME B: BENCHMARK (B), NUMERICAL SOLUTION FOR $\alpha_1 = \alpha_2 = \alpha_4 = \alpha_5 = 2.0$, $\alpha_7 = 0.5$ (N), LINEAR TAYLOR EXTRAPOLATION (T), LINEAR LOGARITHMIC EXTRAPOLATION (L)

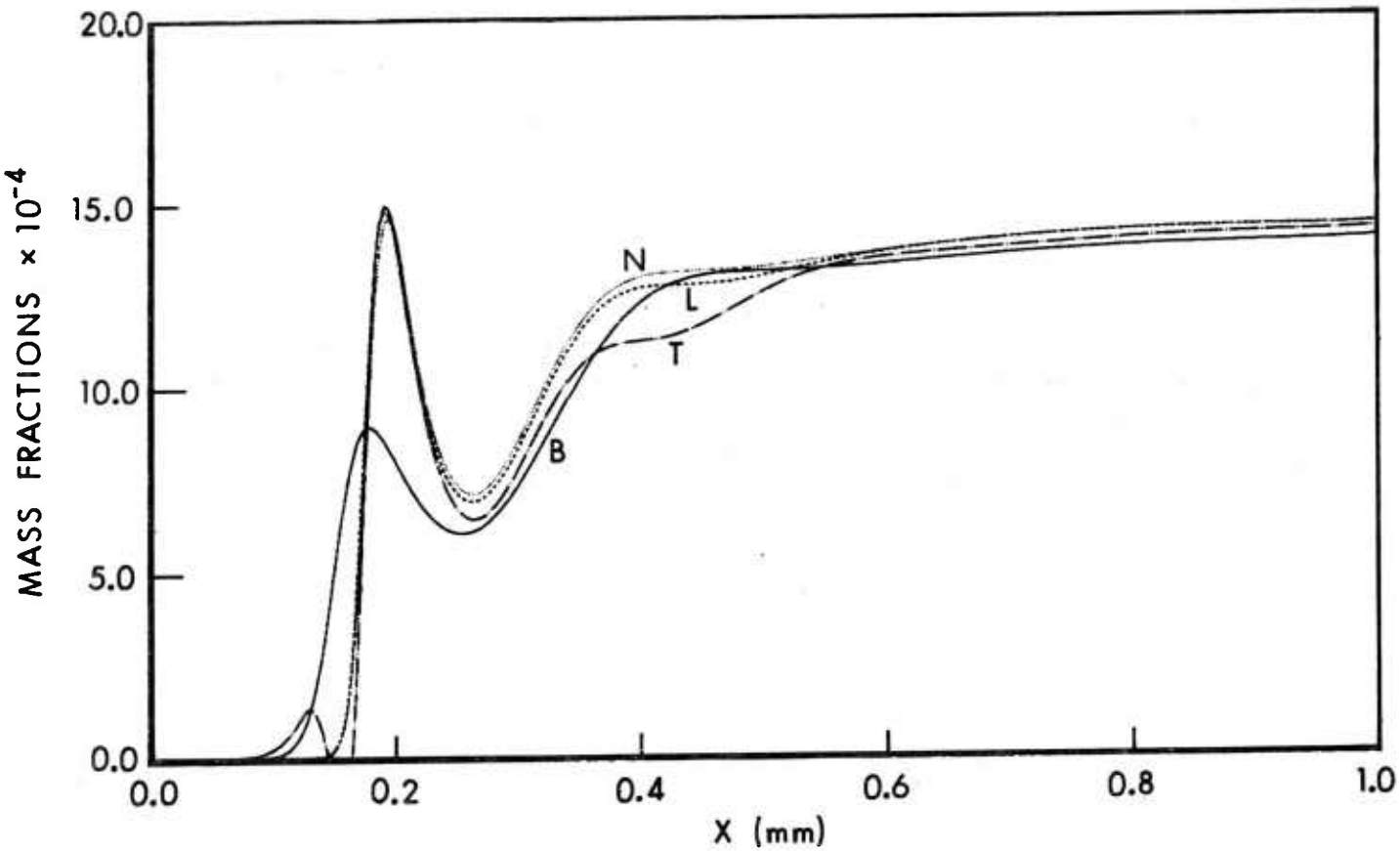

FIGURE 12. CH MASS FRACTION PROFILE, FLAME B: BENCHMARK (B), NUMERICAL SOLUTION FOR $\alpha_1 = \alpha_2 = \alpha_4 = \alpha_5 = 2.0$, $\alpha_7 = 0.5$ (N), SECOND ORDER TAYLOR EXTRAPOLATION (T), SECOND ORDER LOGARITHMIC EXTRAPOLATION (L)

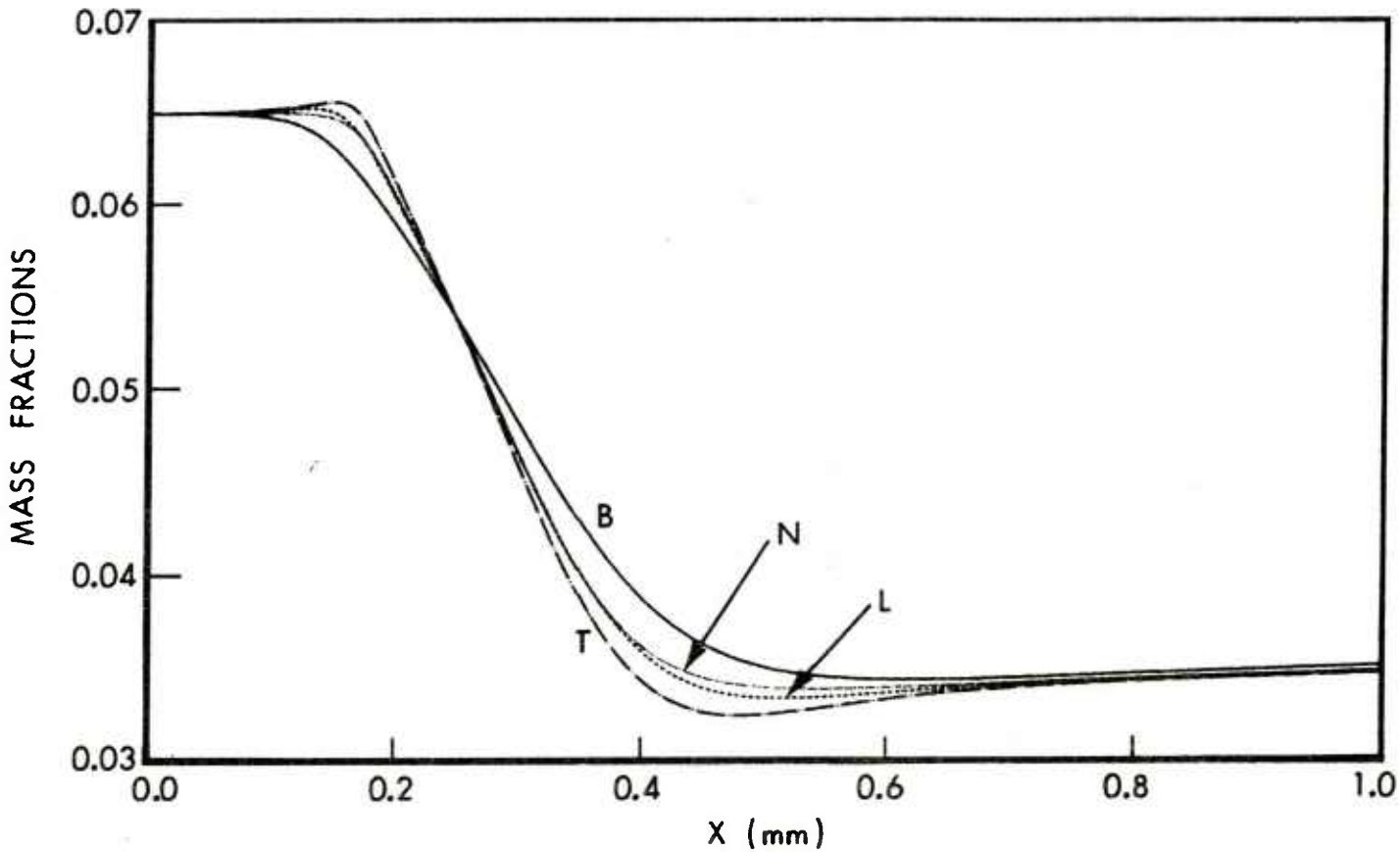

FIGURE 13. H_2 MASS FRACTION PROFILE, FLAME B: BENCHMARK (B), NUMERICAL SOLUTION FOR $\alpha_1 = \alpha_2 = \alpha_4 = \alpha_5 = 2.0$, $\alpha_7 = 0.5$ (N), LINEAR TAYLOR EXTRAPOLATION (T), LINEAR LOGARITHMIC EXTRAPOLATION (L)

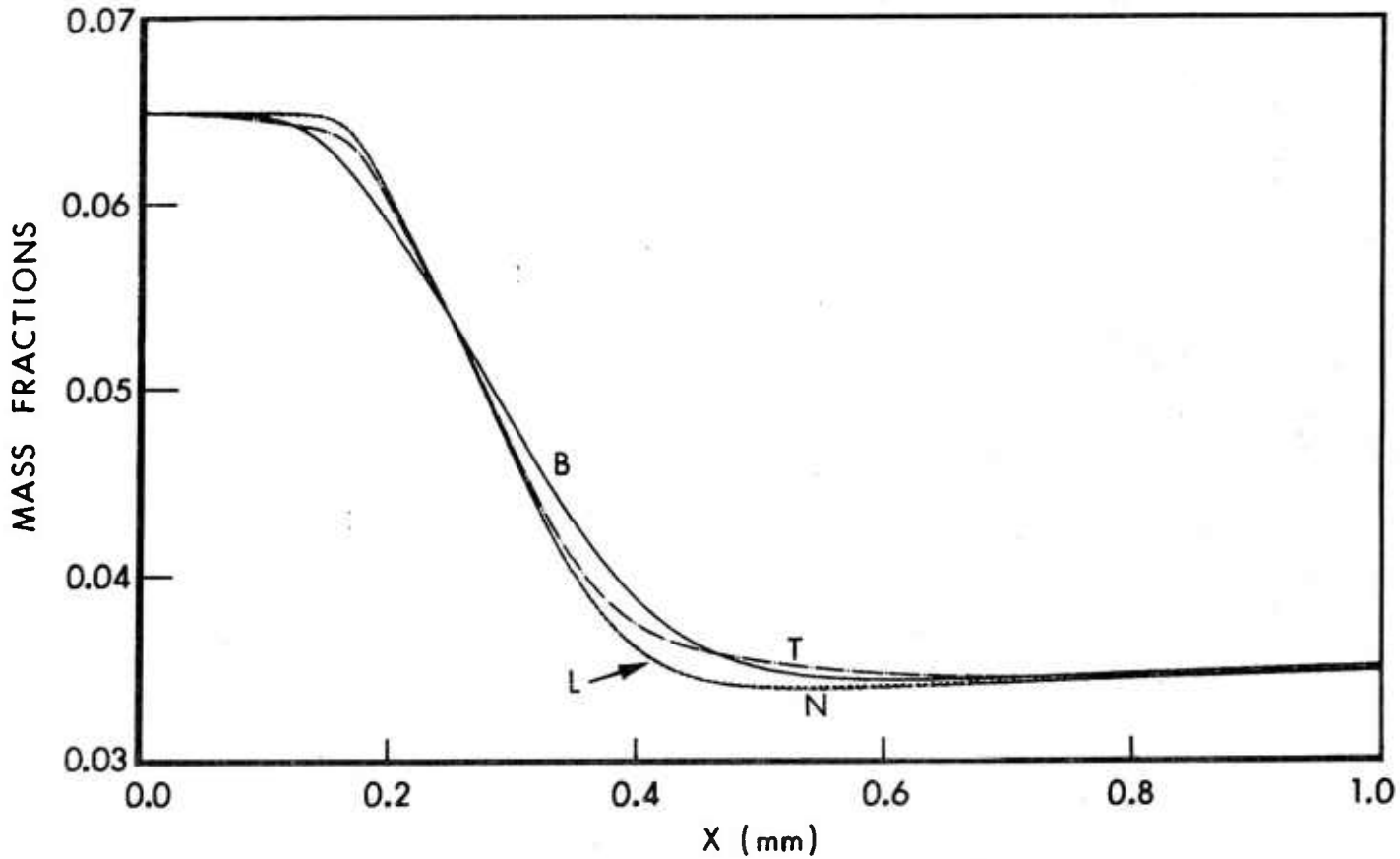

FIGURE 14. H_2 MASS FRACTION PROFILE, FLAME B: BENCHMARK (B), NUMERICAL SOLUTION FOR $\alpha_1 = \alpha_2 = \alpha_4 = \alpha_5 = 2.0$, $\alpha_7 = 0.5$, (N), SECOND ORDER TAYLOR EXTRAPOLATION (T), SECOND ORDER LOGARITHMIC EXTRAPOLATION (L)

solutions.) A more detailed analysis of different parts of the flame can be had by studying the sensitivity coefficient profiles.

The adequacy of the first order formulas was checked qualitatively by computing second order coeffients and quantitatively by comparing the expansion predictions with numerical solutions. For flames with low overall sensitivity, ΣS_E^j, the first order formulas proved adequate for changes up to a factor of two in the variable input parameters. As the overall sensitivity increases, the region of accuracy for the linear expansions decreases. We also found that if ΣS_E^j is not much bigger than 0.5 the logarithmic first order expansion was the more accurate. In any case, the logarithmic expansion was more accurate for the major species and temperature profiles.

Finally, we found that a large value for ΣS_E^j indicated a complex kinetic mechanism while a value close to 0.5 indicated a simple mechanism.

ACKNOWLEDGEMENT

We thank Drs. A.K. Clemins and M.S. Miller for reading this manuscript and making constructive comments.

REFERENCES

1. T.P. Coffee and J.M. Heimerl, "Transport Algorithms for Premixed, Laminar Steady-State Flames," Combustion and Flame, Vol. 43, pp. 273-289, 1981.

2. T.P. Coffee and J.M. Heimerl, "A Method for Computing the Flame Speed for a Laminar, Premixed, One Dimensional Flame," BRL Technical Report, ARBRL-TR-02212, Jan. 1980, AD#A082803.

3. T.P. Coffee, "A Computer Code for the Solution of the Equations Governing a Laminar, Premixed, One Dimensional Flame," BRL Memorandum Report, ARBRL-MR-03165, April 1982, AD#A114041.

4. G. Dixon-Lewis, "Flame Structure and Flame Reaction Kinetics. I. Solution of Conservation Equations and Application to Rich Hydrogen-Oxygen Flames," Proc. Roy. Soc., London A, Vol. 298, pp. 495-513, 1967.

5. R.I. Cukier, C.M. Fortuin, K.E. Shuler, A.G. Petschek, and J.H. Schaibley, "Study of the Sensitivity of Coupled Reaction Systems to Uncertainties in Rate Coefficients I. Theory," J. Chem. Phys., Vol. 59, pp. 3873-3878, 1973.

6. J.H. Schaibly and K.E. Shuler, "Study of the Sensitivity of Coupled Reaction Systems to Uncertainties in Rate Coefficients II. Applications," J. Chem. Phys., Vol. 59, pp. 3879-3888, 1973.

7. R.I. Cukier, J.H. Schaibly, and K.E. Shuler, "Study of the Sensitivity of Coupled Reaction Systems to Uncertainties in Rate Coefficients III. Analysis of the Approximations," J. Chem. Phys., Vol. 63, pp. 1140-1149, 1975.

8. J.T. Hwang, E.P. Dougherty, S. Rabitz and H. Rabitz, "The Green's Function Method of Sensitivity Analysis in Chemical Kinetics," J. Chem. Phys., Vol. 69, pp. 5180-5191, 1978.

9. M. Demiralp and H. Rabitz, "Chemical Kinetic Functional Sensitivity Analysis: Elementary Sensitivities," J. Chem. Phys., Vol. 74, pp. 3362-3375, 1981.

10. P.M. Frank, Introduction to System Sensitivity Theory, Academic Press, 1978.

11. W.C. Gardiner, Jr., "The pC, pR, pP, pM and pS Method of Formulating the Results of Computer Modeling Studies of Chemical Reactions," J. Phys. Chem., Vol. 81, pp. 2367-2371, 1977.

12. G. Dixon-Lewis, "Kinetic Mechanism, Structure and Properties of Premixed Flames in Hydrogen-Oxygen-Nitrogen Mixtures," Proc. R. Soc. London A, Vol. 292, pp., 45-99, 1979.

13. G. Dixon-Lewis, M.M. Sutton, and A. Williams, "Flame Structure and Flame Reaction Kinetics IV. Experimental Investigations of a Fuel-Rich Hydrogen + Oxygen + Nitrogen Flame at Atmospheric Pressure," Proc. Roy. Soc. London A , Vol. 312, pp. 227-234, 1970.

APPENDIX A

INPUT PARAMETERS

APPENDIX A. INPUT PARAMETERS

The enthalpies and heat capacities are evaluated using the sixth order polynomial fits of Gordon and McBride[A1]. These reproduce the JANAF[A2] values to within a few parts per thousand over the temperature range 300K-3000K. The constant c_p is derived from these values (see Reference 1 of text).

The kinetic scheme consists of seventeen reactions and has been taken from Table 9 of Dixon-Lewis (see Reference 12 of text). The rates of the back reactions are computed using the equilibrium constants, which are calculated from the Gordon and McBride polynomial fits. A least squares fit is then made over the range 300K-3000K to obtain the form $k_b = AT^B \exp(-C/T)$.

The transport parameters are given in Table A-2. The values for σ and ε/k are obtained from viscosity measurements.

The viscosities of the individual species and binary diffusion coefficients are calculated as in Reference 1 of the text. The thermal conductivities of the individual species are computed as the average of the Eucken and modified Eucken correction[A3]. The values computed by this procedure are within a few percent of the values computed using the Mason and Monchick formula (as was done in Reference 1 of the text). This simple procedure is used in this paper because it eliminates the necessity of finding the rotational collision numbers of the species, which are not well known.

The constants $\rho^2 D_{im}$ and $\rho\lambda$ are computed from the above transport coefficients, using Method V (see Reference 1 of text).

[A1] *S. Gordon and B.J. McBride, "Computer Program for Calculation of Complex Chemical Equilibrium Compositions, Rocket Performance, Incident and Reflected Shocks and Chapman-Jouguet Detonations," NASA-SP-273, 1971, 1976 program version.*

[A2] *D.R. Stull and H. Prophet, JANAF Thermochemical Tables, 2nd Edition, NSRDS-NBS-37, June 1971.*

[A3] *R.C Reid and J.K. Sherwood, The Properties of Gases and Liquids, 2nd Edition, McGraw Hill, NY., 1966.*

TABLE A-1. REACTIONS AND REACTION RATE PARAMETERS FOR THE H_2-O_2-N_2 SYSTEM

NO	REACTION	A*	B	C
1	$OH+H_2 \rightarrow H_2O+H$	1.17E09**	1.30	-1825
2	$H+O_2 \rightarrow OH+O$	1.42E14	0.00	-8250
3	$O+H_2 \rightarrow OH+H$	1.80E10	1.00	-4480
4	$H+O_2+M' \rightarrow HO_2+M'$	1.03E18	-0.72	0
5	$H+HO_2 \rightarrow OH+OH$	1.40E14	0.00	-540
6	$H+HO_2 \rightarrow O+H_2O$	1.00E13	0.00	-540
7	$H+HO_2 \rightarrow H_2+O_2$	1.25E12	0.00	0
8	$OH+HO_2 \rightarrow H_2O+O_2$	7.50E12	0.00	0
9	$O+HO_2 \rightarrow OH+O_2$	1.40E13	0.00	-540
10	$O+HO_2 \rightarrow OH+O_2$	1.25E12	0.00	0
11	$H+H+H_2 \rightarrow H_2+H_2$	9.20E16	-0.60	0
12	$H+H+N_2 \rightarrow H_2+N_2$	1.00E18	-1.00	0
13	$H+H+O_2 \rightarrow H_2+O_2$	1.00E18	-1.00	0
14	$H+H+H_2O \rightarrow H_2+H_2O$	6.00E19	-1.25	0
15	$H+OH+M'' \rightarrow H_2O+M''$	1.60E22	-2.00	0
16	$H+O+M'' \rightarrow OH+M''$	6.20E16	-0.60	0
17	$OH+OH \rightarrow O+H_2O$	5.7E12	0.00	-390

$[M'] = [H_2] + 0.35\ [O_2] + 6.5\ [H_2O] + 0.44\ [N_2]$

$[M''] = [H_2] + [O_2] + 5.0\ [H_2O] + [N_2]$

* A has units of cm^3/mole-sec for two body reactions or $cm^6/mole^2$-sec for three body reactions. The rate coefficient k is defined by $AT^B exp\ (C/T)$.

**Read 1.17E09 as 1.17×10^9.

TABLE A-2. MOLECULAR PARAMETERS USED FOR THE DETERMINATION OF TRANSPORT PROPERTIES

SPECIES	σ [Å]	ϵ/k [K]	μ [Debye]	α [Å^3]	References
H	2.050	145.0	0	0	A4
O	2.947	127.2	0	0	A5
H_2	2.920	38.0	0	0.79	A4
O_2	3.372	128.7	0	1.60	A5 A3
H_2O	2.600	572.0	1.844	0	A4
N_2	3.620	97.5	0	1.76	A3

OH like O

HO_2 like O_2

[A4] *J. Warnatz, "Calculation of the Structure of Laminar Flat Flames II: Flame Velocity and Structure of Freely Propagating Hydrogen-Oxygen and Hydrogen-Air Flames,"* Ber. Bursenges Phys. Chem., *Vol. 82, pp. 643-649, 1978.*

[A5] *J.M. Heimerl and T.P. Coffee, "The Detailed Modeling of Premixed, Laminar Steady-State Flames I. Ozone,"* Combustion and Flame, *Vol. 39, pp. 301-315, 1980.*

GLOSSARY

C_i concentration of species i, $\rho Y_i/M_i$, mole-cm^{-3}.

c_p specific heat of the mixture, cal-gm^{-1}-K^{-1}.

D_{im} diffusion coefficient for species i into a mixture, cm^2-s^{-1}.

h_i^o specific enthalpy for species i at temperature T_o, cal-gm^{-1}.

h_i specific enthalpy for species i, equals $h^o + c_p\ (T-T_o)$, cal-gm^{-1}.

k_{fr} forward rate for reaction r, cm^3 - mole^{-1}-s^{-1} or cm^6-mole^{-2}-s^{-1}.

k_{br} back rate for reaction r, cm^3-mole^{-1}-s^{-1} or cm^6-mole^{-2}-s^{-1}.

m_o mass flux through the origin in the (ψ,t) coordinate system, gm-cm^{-2}-s^{-1}.

M_i molecular weight of species i, gm-mole^{-1}.

N number of species.

NR number of reactions.

p pressure, atm.

R gas constant = 1.9872 cal-mole^{-1}-K^{-1}.

R_i rate of production of species i by chemical reactions, mole-cm^{-3}-s^{-1}.

R_{ir} rate of production of species i by reaction r, mole -cm^{-3}-s^{-1}.

S burning velocity of the flame, cm-s^{-1}.

S_B benchmark burning velocity, cm-s^{-1}

S_N burning velocity for new values of the input parameters, cm-s^{-1}.

t time, s.

T Temperature, K.

T_o reference temperature for computing enthalpy, K.

T_u temperature of the unburned mixture, K.

T_B temperature of the burned mixture, K.

u_i Y_i if i=1,2...N; T if i=N+1.

v fluid velocity, cm -s^{-1}.

GLOSSARY

$v_{i,r}''$ number of product molecules of species i of reaction r

$v_{i,r}'$ number of reactant molecules of species i of reaction r.

x spatial coordinate, cm.

Y_i mass fraction of species i.

Y_{iu} mass fraction of species i in the unburned mixture.

Y_{iB} mass fraction of species i in the burned mixture.

ψ transformed space coordinate, gm-cm^2.

δ_{ij} Kronecker delta; equals 1 if i=j, equals 0 if $i \neq j$.

λ thermal conductivity of the mixture, cal-cm^{-1}-s^{-1}-K^{-1}.

ρ total gas density, gm-cm^{-3}.

DISTRIBUTION LIST

No. Of Copies	Organization
12	Administrator Defense Technical Info Center ATTN: DTIC-DDA Cameron Station Alexandria, VA 22314
1	Commander US Army Materiel Development and Readiness Command ATTN: DRCDMD-ST 5001 Eisenhower Avenue Alexandria, VA 22333
1	Commander USA ARRADCOM ATTN: DRDAR-TDC D. Gyorog Dover, NJ 07801
2	Commander USA ARRADCOM ATTN: DRDAR-TSS Dover, NJ 07801
1	Commander US Army Armament Materiel Readiness Command ATTN: DRSAR-LEP-L, Tech Lib Rock Island, IL 61299
1	Director USA ARRADCOM Benet Weapons Laboratory ATTN: DRDAR-LCB-TL Watervliet, NY 12189
1	Commander USA Aviation Research and Development Command ATTN: DRDAV-E 4300 Goodfellow Blvd. St. Louis, MO 63120
1	Director USA Air Mobility Research and Development Laboratory Ames Research Center Moffett Field, CA 94035
4	Commander US Army Research Office ATTN: R. Girardelli D. Mann R. Singleton D. Squire Research Triangle Park, NC 27709
1	Commander USA Communications Research and Development Command ATTN: DRDCO-PPA-SA Fort Monmouth, NJ 07703
1	Commander USA Electronics Research and Development Command Technical Support Activity ATTN: DELSD-L Fort Monmouth, NJ 07703
2	Commander USA ARRADCOM ATTN: DRDAR-LCA, D.S. Downs Dover, NJ 07801
2	Commander USA ARRADCOM ATTN: DRDAR-LC, L. Harris DRDAR-LCA, J. Lannon Dover, NJ 07801
1	Commander USA ARRADCOM ATTN: DRDAR-SCA-T, L. Stiefel Dover, NJ 07801
1	Commander USA Missile Command ATTN: DRSMI-R Redstone Arsenal, AL 35898
2	Commander USA Missile Command ATTN: DRSMI-YDL DRSMI-RK, D.J. Ifshin Redstone Arsenal, AL 35898

DISTRIBUTION LIST

No. Of Copies	Organization
1	Commander USA Tank Automotive Research and Development Command ATTN: DRDTA-UL Warren, MI 48090
1	Director USA TRADOC System Analysis Activity ATTN: ATAA-SL, Tech Lib WSMR, NM 88002
1	Office of Naval Research ATTN: R.S. Miller, Code 473 800 N. Quincy Street Arlington, VA 22217
1	Navy Strategic Systems Project Office ATTN: R.D. Kinert, SP 2731 Washington, DC 20360
1	Commander Naval Air Systems Command ATTN: J. Ramnarace, AIR-54111C Washington, DC 20360
3	Commander Naval Ordnance Station ATTN: C. Irish S. Mitchell P.L. Stang, Code 515 Indian Head, MD 20640
1	Commander Naval Surface Weapons Center ATTN: J.L. East, G-23 Dahlgren, VA 22448
1	Commander Naval Surface Weapons Center ATTN: G.B. Wilmot, R-16 Silver Spring, MD 20910
4	Commander Naval Weapons Center ATTN: R.L. Derr, Code 388 China Lake, CA 93555
1	Commander Naval Weapons Center ATTN: T. Boggs China Lake, CA 93555
1	Commander Naval Research Laboratory Washington, DC 20375
1	Commanding Officer Naval Underwater Systems Center Weapons Dept. ATTN: R.S. Lazar/Code 36301 Newport, RI 02840
1	Superintendent Naval Postgraduate School Dept. of Aeronautics ATTN: D.W. Netzer Monterey, CA 93940
6	AFRPL (DRSC) ATTN: R. Geisler D. George B. Goshgarian J. Levine W. Roe D. Weaver Edwards AFB, CA 93523
1	AFATL/DLDL ATTN: O.K. Heiney Eglin AFB, FL 32542
1	AFOSR ATTN: L.H. Caveny Bolling Air Force Base Washington, DC 20332
1	NASA Langley Research Center ATTN: G.B. Northam/MS 168 Hampton, VA 23665

DISTRIBUTION LIST

No. Of Copies	Organization
5	National Bureau of Standards ATTN: J. Hastie M. Jacox T. Kashiwagi H. Semerjian J. Stevenson Washington, DC 20234
1	Aerojet Solid Propulsion Co. ATTN: P. Micheli Sacramento, CA 95813
1	AVCO Everett Rsch. Lab. Div. ATTN: D. Stickler 2385 Revere Beach Parkway Everett, MA 02149
1	Applied Combustion Technology, Inc. ATTN: A.M. Varney 2910 N. Orange Avenue Orlando, FL 32804
2	Atlantic Research Corp. ATTN: M.M. King 5390 Cherokee Avenue Alexandria, VA 22314
1	Battelle Memorial Institute Tactical Technology Center ATTN: J. Huggins 505 King Avenue Columbus, OH 43201
1	Calspan Corporation ATTN: E.B. Fisher P.O. Box 400 Buffalo, NY 14225
2	Exxon Research & Engineering ATTN: A. Dean M. Chou P.O. Box 8 Linden, NJ 07036
1	Ford Aerospace and Communications Corp. ATTN: D. Williams Main Street Ford Road Newport Beach, CA 92663
1	General Electric Company Armament Department ATTN: M.J. Bulman Lakeside Avenue Burlington, VT 05402
1	General Electric Company ATTN: M. Lapp Schenectady, NY 12301
1	General Motors Rsch Labs Physics Department ATTN: J.H. Bechtel Warren, MI 48090
3	Hercules Powder Co. Allegheny Ballistics Lab. ATTN: R.R. Miller P.O. Box 210 Cumberland, MD 21501
3	Hercules, Inc. Bacchus Works ATTN: K.P. McCarty P.O. Box 98 Magna, UT 84044
1	Hercules, Inc. Eglin Operations AFATL/DLDL ATTN: R.L. Simmons Eglin AFB, FL 32542
1	Honeywell, Inc. Defense Systems Division ATTN: D.E. Broden/MS MN-50-2000 600 2nd Street NE Hopkins, MN 55343

DISTRIBUTION LIST

No. Of Copies	Organization
1	IBM Corporation ATTN: A.C. Tam Research Division 5600 Cottle Road San Jose, CA 95193
1	Lawrence Livermore National Laboratory ATTN: C. Westbrook Livermore, CA 94550
1	Lockheed Missiles & Space Co. ATTN: George Lo 3251 Hanover Street Dept. 52-35/B204/2 Palo Alto, CA 94304
2	Los Alamos National Lab Center for Non-Linear Studies ATTN: B. Nichols L. Warner P.O. Box 1663 Los Alamos, NM 87545
1	Shock Hydrodynamics ATTN: W. Anderson 4710-16 Vineland Ave. North Hollywood, CA 91602
1	Olin Corporation Smokeless Powder Operations ATTN: R.L. Cook P.O. Box 222 St. Marks, FL 32355
1	Paul Gough Associates, Inc. ATTN: P.S. Gough P.O. Box 1614 Portsmouth, NH 03801
2	Princeton Combustion Research Laboratories ATTN: M. Summerfield N.A. Messina 1041 US Highway One North Princeton, NJ 08540
1	Pulsepower Systems, Inc. ATTN: L.C. Elmore 815 American Street San Carlos, CA 94070
1	Rockwell International Corp. Rocketdyne Division ATTN: J.E. Flanagan/BA17 6633 Canoga Avenue Canoga Park, CA 91304
2	Sandia National Laboratories Combustion Sciences Dept. ATTN: R. Cattolica D. Stephenson Livermore, CA 94550
1	Science Applications, Inc. ATTN: R. Edelman 23146 Cumorah Crest Woodland Hills, CA 91364
1	Science Applications, Inc. ATTN: H.S. Pergament 1100 State Road, Bldg. N Princeton, NJ 08540
1	Stevens Institute of Tech Davidson Laboratory ATTN: R. McAlevy III Hoboken, NJ 07030
1	Space Sciences, Inc. ATTN: M. Farber Monrovia, CA 91016
4	SRI International ATTN: S. Barker D. Crosley D. Golden Tech Lib 333 Ravenswood Avenue Menlo Park, CA 94025

DISTRIBUTION LIST

No. Of Copies	Organization
1	Teledyne McCormack-Selph ATTN: C. Leveritt 3601 Union Road Hollister, CA 95023
1	Thiokol Corporation Elkton Division ATTN: W.N. Brundige P.O. Box 241 Elkton, MD 21921
3	Thiokol Corporation Huntsville Division ATTN: D.A. Flanagan Huntsville, AL 35807
3	Thiokol Corporation Wasatch Division ATTN: J.A. Peterson P.O. Box 524 Brigham City, UT 84302
1	United Technologies ATTN: A.C. Eckbreth East Hartford, CT 06108
2	United Technologies Corp. ATTN: R.S. Brown R.O. McLaren P.O. Box 358 Sunnyvale, CA 94086
1	Universal Propulsion Company ATTN: H.J. McSpadden Black Canyon Stage 1, Box 1140 Phoenix, AZ 85029
1	Brigham Young University Dept. of Chemical Engineering ATTN: M.W. Beckstead Provo, UT 84601
2	Director Jet Propulsion Laboratory ATTN: L.D. Strand 4800 Oak Grove Drive Pasadena, CA 91103
1	California Institute of Technology ATTN: F.E.C. Culick/ MC 301-46 204 Karman Lab. Pasadena, CA 91125
1	Los Alamos National Lab ATTN: T.D. Butler P.O. Box 1663, Mail Stop B216 Los Alamos, NM 87545
1	University of California, Berkeley Mechanical Engineering Dept. ATTN: J. Daily Berkeley, CA 94720
2	University of California, Santa Barbara Quantum Institute ATTN: K. Schofield M. Steinberg Santa Barbara, CA 93106
1	University of Southern California Dept. of Chemistry ATTN: S. Benson Los Angeles, CA 90007
1	Case Western Reserve Univ. Div. of Aerospace Sciences ATTN: J. Tien Cleveland, OH 44135
1	Cornell University Department of Chemistry ATTN: E. Grant Baker Laboratory Ithaca, NY 14853
1	Univ. of Dayton Rsch Inst. ATTN: D. Campbell AFRPL/PAP Stop 24 Edwards AFB, CA 93523

DISTRIBUTION LIST

No. Of Copies	Organization
1	University of Florida Dept. of Chemistry ATTN: J. Winefordner Gainesville, FL 32601
3	Georgia Institute of Technology School of Aerospace Engineering ATTN: E. Price Atlanta, GA 30332
2	Georgia Institute of Technology School of Aerospace Engineering ATTN: W.C. Strahle B.T. Zinn Atlanta, GA 30332
1	Hughes Aircraft Company ATTN: T.E. Ward 8433 Fallbrook Avenue Canoga Park, CA 91303
1	University of Illinois Dept of Mech Eng ATTN: H. Krier 144 MEB, 1206 W. Green St. Urbana, IL 61801
1	Johns Hopkins University/APL Chemical Propulsion Information Agency ATTN: T.W. Christian Johns Hopkins Road Laurel, MD 20707
1	University of Minnesota Dept. of Mechanical Engineering ATTN: E. Fletcher Minneapolis, MN 55455
4	Pennsylvania State University Applied Research Laboratory ATTN: G.M. Faeth K.K. Kuo H. Palmer M. Micci University Park, PA 16802
1	Polytechnic Institute of NY ATTN: S. Lederman Route 110 Farmingdale, NY 11735
3	Princeton University Forrestal Campus Library ATTN: K. Brezinsky I. Glassman F.A. Williams P.O. Box 710 Princeton, NJ 08540
2	Purdue University School of Aeronautics and Astronautics ATTN: R. Glick J.R. Osborn Grissom Hall West Lafayette, IN 47907
3	Purdue University School of Mechanical Engineering ATTN: N.M. Laurendeau S.N.B. Murthy D. Sweeney TSPC Chaffee Hall West Lafayette, IN 47906
1	Rensselaer Polytechnic Inst. Dept. of Chemical Engineering ATTN: A. Fontijn Troy, NY 12181
1	Southwest Research Institute ATTN: A. B. Wenzel 8500 Culebra Rd. San Antonio, TX 78228

DISTRIBUTION LIST

No. of Copies	Organization
1	Stanford University Dept. of Mechanical Engineering ATTN: R. Hanson Stanford, CA 93106
2	University of Texas Dept. of Chemistry ATTN: W. Gardiner H. Schaefer Austin, TX 78712
1	University of Utah Dept. of Chemical Engineering ATTN: G. Flandro Salt Lake City, UT 84112
1	Virginia Polytechnical Institute State University ATTN: J.A. Schetz Blacksburg, VA 24061

Aberdeen Proving Ground

Dir, USAMSAA
ATTN: DRXSY-D
DRXSY-MP, H. Cohen
Cdr, USATECOM
ATTN: DRSTE-TO-F
Dir, USACSL, Bldg. E3516, EA
ATTN: DRDAR-CLB-PA

USER EVALUATION OF REPORT

Please take a few minutes to answer the questions below; tear out this sheet, fold as indicated, staple or tape closed, and place in the mail. Your comments will provide us with information for improving future reports.

1. BRL Report Number _____

2. Does this report satisfy a need? (Comment on purpose, related project, or other area of interest for which report will be used.)

_____

_____

_____

3. How, specifically, is the report being used? (Information source, design data or procedure, management procedure, source of ideas, etc.) _____

_____

_____

4. Has the information in this report led to any quantitative savings as far as man-hours/contract dollars saved, operating costs avoided, efficiencies achieved, etc.? If so, please elaborate.

_____

_____

5. General Comments (Indicate what you think should be changed to make this report and future reports of this type more responsive to your needs, more usable, improve readability, etc.) _____

_____

_____

_____

6. If you would like to be contacted by the personnel who prepared this report to raise specific questions or discuss the topic, please fill in the following information.

Name: _____

Telephone Number: _____

Organization Address: _____

_____

_____